

Semileptonic B_c decays to P-wave charmonia in the light-cone QCDSR

Tarik Akan^{a,b*}, Elif Cincioglu^{c†}, Altug Ozpineci^{c‡} and Adnan Tegmen^{b§}

^a*Physics Department, Yozgat Bozok University, 66100 Yozgat, Turkey*

^b*Physics Department, Ankara University, 06100 Ankara, Turkey*

^c*Physics Department, Middle East Technical University, 06800 Ankara, Turkey*

March 28, 2023

Abstract

B_c mesons are laboratories for probing heavy quark physics. Furthermore, they decay into charmonia and hence their decays can be used to analyze possible exotic charmonium. In this work, the semileptonic decays of B_c mesons into P wave charmonia are analysed using light cone QCD sum rules (LCSR). The distributions amplitudes for the charmonia are taken from a quark model computation. The obtained decay rates for the ground state and excited charmonia are compared with the results found in the literature.

*tarik.akan@bozok.edu.tr

†elifcincioglu@gmail.com

‡ozpineci@metu.edu.tr

§tegmen@science.ankara.edu.tr

1 Introduction

In the past several decades, many particle physicists devoted themselves to explain composite quark systems, the so-called hadrons, and checked predictions of quantum chromodynamics. Many models are developed in perturbative and non-perturbative domains for this purpose. During the last few decades, heavy flavoured hadron research has become very popular in hadron physics since many charmonium-like states have been discovered at B-factories. Among these states, some of them may not be simple quark and anti-quark states. They could be more complex structures, the so-called exotic states, such as tetraquarks, pentaquarks, meson molecules, etc. Therefore, there is not a certain hadron structure. The possible meson states which include the b quarks, are the hidden b quark states, the so-called $\Upsilon(b\bar{b})$ and the open b quark states, which are called B mesons ($b\bar{q}$, where $q = u, d, s, c$). Among the B mesons, B_c meson ($b\bar{c}$) is a very interesting particle due to its two different kind of heavy quark constituents and final states of some of its decays contain a $c\bar{c}$ pair [1, 2]. The decays and spectroscopy of B_c mesons are described by various QCD models, which can be tested at B-factories. Due to small velocities of constituent quarks in heavy quarkonia and B_c mesons, the mesons can be treated as non-relativistic systems. Many non-relativistic potential models claim that the b and \bar{c} are tightly bound in a very compact system and have a rich spectroscopy of excited states [3]. Investigation of these excited states also increases the popularity of B_c states. Since the first successful observation of B_c in CDF at Tevatron, Fermilab in the interaction $B_c \rightarrow J/\psi l \bar{\nu}_l$ [4], there has been remarkable progress in the study of semileptonic and nonleptonic B meson decays [5–14]. Besides the OZI suppressed decay channels, in which the b and \bar{c} annihilate, B_c meson can also decay due to the decay of one of its constituents. If the final quark is a light quark, the final state is a D or a B meson depending on which constituent decays. If the b quark decays into a c quark, than the final state contains a charmonium. Its weak decay channel shows us a large branching ratio to final states containing a J/ψ . It has been pointed out that [11–17], due to its unique nature, the decays of B_c meson can be used to extract the magnitudes and phases of CKM matrix elements. Additionally, if the final state contains a $c\bar{c}$ pair, the decay can be used to probe hidden charm exotic states. For example, the produced $c\bar{c}$ state can couple directly or through a $D\bar{D}^*/\bar{D}\bar{D}^*$ loop to X(3872) [18–21].

Due to the non-perturbative nature of QCD [22–25], to investigate the semileptonic decays of B_c meson, a non-perturbative method is needed. QCD sum rules (QCDSR) and its variations like the Light Cone QCDSR have been used successfully to analyze the properties of hadrons. In the sum rules analysis, the properties of low lying states can be easily extracted but the question of studying the properties of excited states is still an open problem. For this reason, e.g. in [26, 27, 55], only the decays of B_c into ground state P-wave charmonia has been analyzed. In X(3872), if it contains any charmonium components, it is expected to be the first radial excitation [28]. Hence if B_c meson decays will be used to probe the structure of possible exotic states like X(3872) it is important to study decays into final states that contain the radial excitations. In [29], light cone DAs are related to the quark model wave functions. In [30, 31] this relation is used to calculate the DAs describing the ground state and radially excited P-wave charmonia. In this work, in order to study the decays of B_c mesons into P-wave charmonia, the results of [30, 31] are used.

In section 2 the procedure is explained in more detail. Important parameters of LCSR and a mass prediction for B_c are discussed and presented in the section 3. Then the obtained numerical results for decay rate and branching fractions, including their excited states are

presented in section 4 and compared with existing results in the literature. Finally, our conclusion is given in the section 5.

2 Form Factor Calculation with LCSR

The $B_c \rightarrow (c\bar{c}) l \bar{\nu}_l$ decays proceed via the $b \rightarrow c$ transition at the quark level fig. 1. This transition is described by the effective Hamiltonian: [27, 33, 36]

$$H_{eff} = \frac{G_F}{\sqrt{2}} V_{cb} J_{lep}^\mu J_\mu^{had}, \quad (1)$$

where G_F is the Fermi constant, V_{cb} is the CKM matrix element for the $b \rightarrow c$ transition, and the currents are given by $J_{lep}^\mu = \bar{l} \gamma^\mu (\mathbb{1} - \gamma_5) \nu_l$ and $J_\mu^{had} = \bar{c} \gamma_\mu (\mathbb{1} - \gamma_5) b$. The transition matrix element of the decay can be obtained by sandwiching the effective Hamiltonian between corresponding initial and final states, which becomes after factoring out the hadronic and leptonic parts

$$M = \frac{G_F}{\sqrt{2}} V_{cb} \langle l \bar{\nu}_l | \bar{l} \gamma_\mu (\mathbb{1} - \gamma_5) \nu_l | 0 \rangle \langle c \bar{c}(p') | \bar{c} \gamma_\mu (\mathbb{1} - \gamma_5) b | B_c(p) \rangle, \quad (2)$$

where B_c is the initial pseudoscalar B_c meson and the final $c\bar{c}$ state can be a scalar (S), axial-vector(A) or a tensor(T) charmonium. The matrix elements $\langle c \bar{c} | \bar{c} \gamma_\mu (\mathbb{1} - \gamma_5) b | B_c(p) \rangle$ for each possibility can be parameterized in terms of form factors as follows [27, 32, 33]:

$$\langle S^n(p') | \bar{c} \gamma_\mu (\mathbb{1} - \gamma_5) b | B_c(p) \rangle = f_1^n(q^2)(p' + p)_\mu + f_2^n(q^2)(p - p')_\mu, \quad (3)$$

$$\langle A^n(p', \varepsilon) | \bar{c} \gamma_\mu (\mathbb{1} - \gamma_5) b | B_c(p) \rangle = \frac{i f_V^n(q^2)}{(m_{B_c} + m_A)} \varepsilon_{\mu\rho\alpha\beta} \varepsilon^{*\rho} p^\alpha p'^\beta \quad (4)$$

$$+ i \left[f_{V_0}^n(q^2)(m_{B_c} + m_A) \varepsilon_\mu^* - \frac{f_{V_+}^n(q^2)}{(m_{B_c} + m_A)} (\varepsilon^* p)(p' + p)_\mu \right. \\ \left. - \frac{f_{V_-}^n(q^2)}{(m_{B_c} + m_A)} (\varepsilon^* p)(p - p')_\mu \right],$$

$$\langle T^n(p', \varepsilon) | \bar{c} \gamma_\mu (\mathbb{1} - \gamma_5) b | B_c(p) \rangle = \frac{2 i f_T^n(q^2)}{m_{B_c} + m_T} \varepsilon_{\mu\rho\alpha\beta} \varepsilon_{\rho\sigma}^* \frac{p^\sigma}{m_{B_c}} p_\alpha p'_\beta \quad (5)$$

$$+ i \left[f_{T_0}^n(q^2)(m_{B_c} + m_T) \varepsilon^{*\mu\alpha} \frac{p^\alpha}{m_{B_c}} \right. \\ \left. - f_{T_+}^n(q^2) p^\mu \varepsilon_{\alpha\beta}^* \frac{p^\alpha p^\beta}{m_{B_c}^2} - f_{T_-}^n(q^2) p'^\mu \varepsilon_{\alpha\beta}^* \frac{p^\alpha p^\beta}{m_{B_c}^2} \right],$$

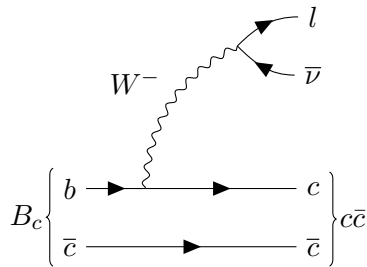


Figure 1: Feynman diagram corresponding to the semileptonic decay $B_c \rightarrow (c\bar{c}) l \bar{\nu}$

where n is the radial excitation quantum number of the charmonium, f_1^n and f_2^n are the form factors for the scalar; f_V^n , $f_{V_0}^n$, $f_{V_+}^n$ and $f_{V_-}^n$ are the form factors, m_A is the mass and ϵ_μ is the polarization vector of the axial-vector; f_T^n , $f_{T_0}^n$, $f_{T_+}^n$, and $f_{T_-}^n$ are the form factors, m_T is the mass and $\epsilon_{\mu\nu}$ the polarization tensor of the tensor P-wave charmonium.

To obtain the form factors within the LCSR framework, a suitably chosen correlation function is studied. In this work, the correlator is chosen to be:

$$\Pi_\mu = i \int d^4x e^{ipx} \langle c\bar{c}(p') | T\{j_\mu^W(0) j_B^\dagger(x)\} | 0 \rangle. \quad (6)$$

where $j_\mu^W = \bar{c}\gamma_\mu(\mathbb{1} - \gamma_5)b$ is the weak current responsible for the $b \rightarrow c$ transition and j_B^\dagger is an operator that can create a B_c meson from the vacuum. In this work j_B is chosen as $j_B = \bar{c}\gamma_5 b$. Hence the correlation function can be written as

$$\Pi_\mu = i \int d^4x e^{ipx} \langle c\bar{c}(p') | T\{\bar{c}(0) \gamma_\mu(\mathbb{1} - \gamma_5) b(0) \bar{b}(x) \gamma_5 c(x)\} | 0 \rangle. \quad (7)$$

The main idea behind LCSR method is to write the correlation function eq. (7) in terms of both the QCD degrees of freedom and light cone DAs, so called the QCD representation, and also in terms of the properties of the hadrons, so called the phenomenological representation. In the kinematical region $p^2 > 0$, the correlation can be written in terms of hadronic parameters. To obtain this hadronic representation, a resolution of identity in terms of the hadronic states is inserted between the interpolating currents. In the hadronic representation, the correlation function can be written as:

$$\Pi_\mu^{phen.}(p^2) = \sum_h \frac{\langle c\bar{c}(p') | \bar{c}\gamma_\mu(\mathbb{1} - \gamma_5) b | h \rangle \langle h | \bar{b}\gamma_5 c | 0 \rangle}{m_h^2 - p^2} + \dots, \quad (8)$$

where the sum is over all single hadron states, h , for which $\langle h | \bar{b}\gamma_5 c | 0 \rangle \neq 0$, and \dots represents the contributions from multi hadronic states and continuum. Note that in eq. (8), there is no sum over $c\bar{c}$ states as these states are parametrized by their distribution amplitudes. This allows one to study the properties of excited $c\bar{c}$ states if their distribution amplitudes are known. Separating out the contribution of the lowest mass state, the correlation function can be written as

$$\Pi_\mu^{phen.}(p^2) = \frac{\langle c\bar{c}(p') | \bar{c}(0) \gamma_\mu(\mathbb{1} - \gamma_5) b(0) | B_c(0^-) \rangle \langle B_c(0^-) | \bar{b}(0) \gamma_5 c(0) | 0 \rangle}{m_{B_c}^2 - p^2}. \quad (9)$$

where the contribution from the higher B_c mesons and the continuum are omitted. The matrix element $\langle B_c(0^-) | \bar{b}(0) \gamma_5 c(0) | 0 \rangle$ can be written in terms of the leptonic decay constant of B_c as:

$$\langle B_c(0^-) | \bar{b}(0) \gamma_5 c(0) | 0 \rangle = -\frac{if_{B_c} m_{B_c}^2}{m_b + m_c}, \quad (10)$$

where f_{B_c} is the leptonic decay constant of B_c meson.

Using the definition of the remaining matrix elements in terms of the form factors given in eqs. (3) to (5), the phenomenological representation of the correlation function becomes:

- For spin-0 charmonium states;

$$\begin{aligned} \Pi_\mu^{phen.}(p^2) &= \frac{i}{m_{B_c}^2 - p^2} (f_1^n(q^2)(p' + p)_\mu + f_2^n(q^2)(p - p')_\mu) \frac{f_{B_c} m_{B_c}^2}{m_b + m_c} \\ &\equiv i(p' + p)_\mu \Pi_{f_1^n}^{phen.} + i(p - p')_\mu \Pi_{f_2^n}^{phen.} \end{aligned} \quad (11)$$

- For spin-1 charmonium states;

$$\begin{aligned}
\Pi_{\mu}^{phen}(p^2) &= \frac{i}{m_{B_c}^2 - p^2} \left\{ \frac{if_V^n(q^2)}{(m_{B_c} + m_A)} \varepsilon_{\mu\rho\alpha\beta} \varepsilon^{*\rho} p^\alpha p'^\beta \right. \\
&\quad + i \left[f_{V_0}^n(q^2)(m_{B_c} + m_A) \varepsilon_\mu^* - \frac{f_{V_+}^n(q^2)}{(m_{B_c} + m_A)} (\varepsilon^* p)(p' + p)_\mu \right. \\
&\quad \left. \left. - \frac{f_{V_-}^n(q^2)}{(m_{B_c} + m_A)} (\varepsilon^* p)(p - p')_\mu \right] \right\} \frac{f_{B_c} m_{B_c}^2}{m_b + m_c} \\
&\equiv \varepsilon_{\mu\rho\alpha\beta} \varepsilon^{*\rho} p^\alpha p'^\beta \Pi_{f_V^n}^{phen} + \varepsilon_\mu^* \Pi_{f_{V_0}^n}^{phen} - (\varepsilon^* p)(p' + p)_\mu \Pi_{f_{V_+}^n}^{phen} \\
&\quad - (\varepsilon^* p)(p - p')_\mu \Pi_{f_{V_-}^n}^{phen}
\end{aligned} \tag{12}$$

- For spin-2 charmonium states;

$$\begin{aligned}
\Pi_{\mu}^{phen}(p^2) &= \frac{i}{m_{B_c}^2 - p^2} \left\{ \frac{2if_T^n(q^2)}{m_{B_c} + m_T} \varepsilon_{\mu\rho\alpha\beta} \varepsilon_{\rho\sigma}^* \frac{p^\sigma}{m_{B_c}} p_\alpha p'_\beta \right. \\
&\quad + i \left[f_{T_0}^n(q^2)(m_{B_c} + m_T) \varepsilon_{\mu\alpha}^* \frac{p^\alpha}{m_{B_c}} \right. \\
&\quad \left. - f_{T_+}^n(q^2)(p + p')_\mu \varepsilon_{\alpha\beta}^* \frac{p^\alpha p^\beta}{m_{B_c}^2} - f_{T_-}^n(q^2)(p - p')_\mu \varepsilon_{\alpha\beta}^* \frac{p^\alpha p^\beta}{m_{B_c}^2} \right] \right\} \frac{f_{B_c} m_{B_c}^2}{m_b + m_c} \\
&\equiv \varepsilon_{\mu\rho\alpha\beta} \varepsilon_{\rho\sigma}^* p^\sigma p_\alpha p'_\beta \Pi_{f_T^n}^{phen} + \varepsilon_{\mu\alpha}^* \Pi_{f_{T_0}^n}^{phen} - (p + p')_\mu \varepsilon_{\alpha\beta}^* p^\alpha p^\beta \Pi_{f_{T_+}^n}^{phen} \\
&\quad - (p - p')_\mu \varepsilon_{\alpha\beta}^* p^\alpha p^\beta \Pi_{f_{T_-}^n}^{phen}
\end{aligned} \tag{13}$$

where the coefficients of certain Dirac structures in eqs. (3) to (5) are defined as:

$$\Pi_{f_X^n}^{phen} = \frac{if_X^n}{m_{B_c}^2 - p^2} \kappa_{f_X^n} \tag{14}$$

where f_X^n are formfactors and $\kappa_{f_X^n}$ are constants for each form factor f_X^n are defined as

$$\kappa_{f_1^n} = \kappa_{f_2^n} = \frac{f_{B_c} m_{B_c}^2}{m_b + m_c} \tag{15}$$

$$\kappa_{f_V^n} = -\frac{1}{m_{B_c} + m_A} \frac{f_{B_c} m_{B_c}^2}{m_b + m_c} \tag{16}$$

$$\kappa_{f_{V_0}^n} = -(m_{B_c} + m_A) \frac{f_{B_c} m_{B_c}^2}{m_b + m_c} \tag{17}$$

$$\kappa_{f_{V_+}^n} = \kappa_{f_{V_-}^n} = -\frac{1}{m_{B_c} + m_A} \frac{f_{B_c} m_{B_c}^2}{m_b + m_c} \tag{18}$$

$$\kappa_{f_T^n} = -\frac{2}{(m_{B_c} + m_T)} \frac{f_{B_c} m_{B_c}}{m_b + m_c} \tag{19}$$

$$\kappa_{f_{T_0}^n} = -(m_{B_c} + m_T) \frac{f_{B_c} m_{B_c}}{m_b + m_c} \tag{20}$$

$$\kappa_{f_{T_+}^n} = \kappa_{f_{T_-}^n} = -\frac{f_{B_c}}{m_b + m_c} \tag{21}$$

The various form factors f_X^n can be obtained in terms of the QCD parameters once $\Pi_{f_X^n}$ is expressed in terms of these parameters and the two representations of $\Pi_{f_X^n}$ are matched.

In the kinematical region when p^2 is both large and negative, i.e. the deep Euclidean region, the correlation function can be calculated in terms of QCD parameters. To calculate Π_μ in terms of the QCD parameters, the first step is to contract the b quark fields and eq. (7) is expressed as:

$$\begin{aligned}\Pi_\mu(p^2) &= i \int d^4x e^{ipx} \langle c\bar{c}(p') | \bar{c}(0) \gamma_\mu (\mathbb{1} - \gamma_5) \overline{b(0)} b(x), \gamma_5 c(x) | 0 \rangle \\ &= i \int d^4x e^{ipx} \langle c\bar{c}(p') | \bar{c}(0) \gamma_\mu (\mathbb{1} - \gamma_5) iS_b(x) \gamma_5 c(x) | 0 \rangle,\end{aligned}\quad (22)$$

where the heavy quark propagator is defined as

$$S_Q(x) = \frac{m_Q^2}{4\pi^2} \left[\frac{i\cancel{x}}{(-x^2)} K_2(m_Q \sqrt{-x^2}) + \frac{1}{(\sqrt{-x^2})} K_1(m_Q \sqrt{-x^2}) \right]. \quad (23)$$

where the $K_n(m_Q \sqrt{-x^2})$ ($n = 1$ or 2) are the modified Bessel functions. Using the Fierz identity, this expression of the correlation function can be written as:

$$\Pi_\mu(p^2) = \sum_{\Gamma} \frac{i}{4} \int d^4x e^{ipx} \langle c\bar{c}(p') | \bar{c}(0) \Gamma c(x) | 0 \rangle \text{Tr}[\gamma_\mu (\mathbb{1} - \gamma_5) S_b(x) \gamma_5 \Gamma] \quad (24)$$

where Γ is summed over the Dirac basis for gamma matrices: $\{\mathbb{1}, \gamma_5, \gamma_\mu, i\gamma_\mu\gamma_5, \frac{\sigma_{\mu\nu}}{\sqrt{2}}\}$. The matrix elements appearing in eq. (24) can be written in terms of the distribution amplitudes of the corresponding $c\bar{c}$ state under study. The leading twist contributions have been calculated in [30, 31]. Note that, due to kinematical enhancements, higher twist DA's can receive large contribution that can be expressed in terms of the leading twist DAs using Wandrupa-Wilczek like relations. The non-zero matrix elements can be written as [30]:

$$\langle S^n(P) | \bar{c}(0) \gamma^\mu c(x) | 0 \rangle = f_S^n \int_0^1 du e^{-i\bar{u}px} \left[p^\mu \phi_S^n(u) + x^\mu \frac{m_S^2}{2px} g_s(u) \right], \quad (25)$$

$$\begin{aligned}\langle A^n(P, \varepsilon_{\lambda=0}) | \bar{c}(0) \gamma^\mu \gamma_5 c(x) | 0 \rangle &= -i f_A^n m_A \int_0^1 du e^{-i\bar{u}px} \left\{ p^\mu \frac{\varepsilon x}{px} \phi_{A\parallel}^n(u) + \varepsilon_\perp^\mu g_{A\perp}(u) \right. \\ &\quad \left. - x^\mu \frac{\varepsilon x}{2(px)^2} m_A^2 g_{A3}(u) \right\},\end{aligned}\quad (26)$$

$$\begin{aligned}\langle A^n(P, \varepsilon_{\lambda=\pm 1}) | \bar{c}(0) \sigma^{\mu\nu} \gamma_5 c(x) | 0 \rangle &= f_{A\perp}^n \int_0^1 du e^{-i\bar{u}px} \left\{ (\varepsilon_\perp^\mu p^\nu - \varepsilon_\perp^\nu p^\mu) \phi_{A\perp}^n(u) \right. \\ &\quad + (p^\mu x^\nu - p^\nu x^\mu) \frac{m_A^2 \varepsilon x}{(px)^2} h_{A\parallel}(u) \\ &\quad \left. + (\varepsilon_\perp^\mu x^\nu - \varepsilon_\perp^\nu x^\mu) \frac{m_A^2}{2px} h_{A3}(u) \right\},\end{aligned}\quad (27)$$

$$\langle T^n(P, \varepsilon_{\lambda=0}) | \bar{c}(0) \gamma^\mu c(x) | 0 \rangle = f_T^n m_T^2 \int_0^1 du e^{-i\bar{u} p \cdot x} \left\{ p^\mu \frac{\varepsilon^{\bullet\bullet}}{(px)^2} \phi_{T\parallel}^n(u) + \frac{\varepsilon_\perp^{\mu\bullet}}{px} g_{T\perp}(u) - x^\mu \frac{\varepsilon^{\bullet\bullet}}{2(px)^3} m_T^2 g_{T_3}(u) \right\}, \quad (28)$$

$$\begin{aligned} \langle T^n(P, \varepsilon_{\lambda=\pm 1}) | \bar{c}(0) \sigma^{\mu\nu} c(x) | 0 \rangle &= -i f_T^n m_T \int_0^1 du e^{-i\bar{u} p \cdot x} \left\{ \frac{\varepsilon_\perp^{\mu\bullet} p^\nu - \varepsilon_\perp^{\nu\bullet} p^\mu}{px} \phi_{T\perp}^n(u) \right. \\ &\quad + (p^\mu x^\nu - p^\nu x^\mu) \frac{m_T^2 \varepsilon^{\bullet\bullet}}{(px)^3} h_{T\parallel}(u) \\ &\quad \left. + (\varepsilon_\perp^{\mu\bullet} x^\nu - \varepsilon_\perp^{\bullet\nu} x^\mu) \frac{m_T^2}{2(px)^2} h_{T_3}(u) \right\}, \end{aligned} \quad (29)$$

where

$$p^\mu = P^\mu - x^\mu \frac{m_H^2}{2Px} \quad (30)$$

where m_H is the charmonium mass in question. The subleading twist DAs that receive large contributions are also included, $\bar{u} = 1 - u$ and S, A, T correspond to scalar, axial-vector and tensor, respectively. The large contributions to the subleading twist DAs can be calculated as [50–52]:

$$g_S(u) \simeq \frac{1}{2} \left[\int_0^u dv \frac{\phi_S(v)}{\bar{v}} + \int_u^1 dv \frac{\phi_S(v)}{v} \right], \quad (31)$$

$$g_{A\perp}(u) \simeq \frac{1}{2} \left[\int_0^u dv \frac{\phi_{A\parallel}(v)}{\bar{v}} + \int_u^1 dv \frac{\phi_{A\parallel}(v)}{v} \right], \quad (32)$$

$$g_{T\perp}(u) \simeq \int_0^u dv \frac{\phi_{T\parallel}(v)}{\bar{v}} + \int_u^1 dv \frac{\phi_{T\parallel}(v)}{v}, \quad (33)$$

$$h_{A\parallel}(u) \simeq 2 \left[\bar{u} \int_0^u dv \frac{\phi_{A\perp}(v)}{\bar{v}} + u \int_u^1 dv \frac{\phi_{A\perp}(v)}{v} \right], \quad (34)$$

$$h_{T\parallel}(u) \simeq (2u - 1) \left[\int_0^u dv \frac{\phi_{T\perp}(v)}{\bar{v}} + \int_u^1 dv \frac{\phi_{T\perp}(v)}{v} \right]. \quad (35)$$

Note that in eqs. (31) to (35), only contributions to DAs appearing in our final results are presented. The polarization vector of the axial-vector meson is separated into longitudinal and transverse parts as

$$\varepsilon_\perp^\mu = \varepsilon^\mu - \varepsilon_\parallel^\mu, \quad \varepsilon_\parallel^\mu = \frac{\varepsilon x}{px} \left(p^\mu - x^\mu \frac{M_H^2}{2px} \right). \quad (36)$$

On the other hand, for the tensor meson, polarization tensor is similarly described in the following way

$$\varepsilon_\perp^{\mu\bullet} = \varepsilon^{\mu\bullet} - \varepsilon_\parallel^{\mu\bullet}, \quad \varepsilon_\parallel^{\mu\bullet} = \frac{\varepsilon^{\bullet\bullet}}{px} \left(p^\mu - x^\mu \frac{M_H^2}{2px} \right), \quad (37)$$

where $\varepsilon_{\mu\bullet} = \varepsilon^{\mu\nu} x_\nu$. It should be noted that there is no contribution to the matrix elements of mesons with polarizations $\lambda = \pm 2$ from the leading twist [53,56]. Depending on the C parities of the $c\bar{c}$ states, the distribution amplitudes are odd or even under the $u \leftrightarrow \bar{u}$ exchange. ϕ_S ,

$\phi_{T\parallel}$, and $\phi_{T\perp}$ are odd under the $u \leftrightarrow \bar{u}$ transform since the scalar and tensor P-wave charmonia have positive C-parities. However, there are two axial P-wave charmonia: one C-odd and the other C-even. In the case of C-even axial vector mesons, $\phi_{A\parallel}$, $\phi_{A\perp}$ wave functions are even and odd, respectively and vice versa for the C-odd axial-vector mesons.

Once these non-local matrix elements are defined, the correlation function can be expressed in terms of the distributions amplitudes after a straightforward computation. From this expression, taking the coefficients of various Dirac structures, one can obtain expression of the function $\Pi_{f_X}^{QCD}$ in terms of the QCD parameters.

The expressions for the function Π_{f_X} obtained in the two kinematical regions, $p^2 > 0$ and p^2 in the deep Euclidean region, are matched using the spectral representation of the correlation function. In general, the correlation function, or more precisely the coefficient of any of the Dirac structures appearing in the correlation function can be written as

$$\Pi(q^2, p^2) = \int_0^\infty ds \frac{\rho(q^2, s)}{s - p^2} + \text{polynomials in } p^2. \quad (38)$$

where ρ is called the spectral density. To get rid of the polynomials and suppress the contribution of higher states and continuum, Borel transformation is carried out, after which one obtains:

$$f_X^n \kappa_{f_X^n} e^{-\frac{m_{B_c}^2}{M^2}} + \dots = \int_0^\infty ds \rho_{f_X^n}^{QCD}(q^2, s) e^{-\frac{s}{M^2}}. \quad (39)$$

where \dots represents the contribution of the higher states and continuum. To model and subtract the contributions of higher states and the continuum, quark hadron duality is used. It is assumed that above a threshold value of s_0 , ρ^{phen} and ρ^{QCD} are equal to each other:

$$\rho_{f_X^n}^{\text{higher states}}(q^2, s) = \rho_{f_X^n}^{QCD}(q^2, s) \theta(s - s_0) \quad (40)$$

where s_0 is called the threshold value.

Eventually, the light cone sum rules prediction for the form factors can be obtained from:

$$f_X^n(q^2) e^{-\frac{m_{B_c}^2}{M^2}} = \frac{1}{\kappa_{f_X^n}} \int_0^{s_0} ds \rho^{QCD}(q^2, s) e^{-\frac{s}{M^2}} \quad (41)$$

The analytical results for the form factors are presented in appendix A.

3 Numerical Analysis for Form Factors

In order to obtain the numerical values for the right hand side of eq. (41), the values of the quark masses, explicit expression of LCDA's, the masses of the $c\bar{c}$ states and the mass of the B_c meson are needed. For the quark masses, the following pole masses are used: [47, 48] $m_b = 4.78$ GeV, $m_c = 1.67$ GeV. The distribution amplitudes for the ground state and the next two excited states of the P-wave charmonium are modeled in [31, 56] as

$$\phi_{odd}^{n=1}(u) = a(1 - u^2)^2 \left[E_3 \left[\frac{\beta}{1 - u^2} \right] + b \exp \left(-\frac{u^2}{c} \right) \right] \quad (42)$$

$$\phi_{odd}^{n=2,3}(u) = a \left[\frac{1}{1 + \frac{(u^2 - u_0^2)^2}{\sigma^2}} + b \exp \left(-\frac{u^2}{c} \right) \right] \exp \left(-\frac{\beta}{1 - u^2} \right) \quad (43)$$

Masses (GeV)	$n = 1$	$n = 2$	$n = 3$
$m_S ({}^3P_0)$	3.37	3.88	4.30
$m_A ({}^3P_1)$	3.54	3.97	4.33
$m_A ({}^1P_1)$	3.53	3.96	4.37
$m_T ({}^3P_2)$	3.54	3.98	4.34

Table 1: Quark model masses calculated for the first three levels of charmonia [31]

$$\phi_{even}^{n=1}(u) = a u(1-u^2) \left[\exp\left(\frac{\beta}{1-u^2}\right) + b \exp\left(-\frac{u^2}{c}\right) \right] \quad (44)$$

$$\phi_{even}^{n=2,3}(u) = -\frac{d}{du} \left\{ a \left[\frac{1}{1+\frac{(u^2-u_0^2)^2}{\sigma^2}} + b \exp\left(-\frac{u^2}{c}\right) \right] \exp\left(-\frac{\beta}{1-u^2}\right) \right\} \quad (45)$$

where a , b , c , β , σ^2 , and u_0 are numerical parameters whose values are presented in [31]. In general LCDA's are scale dependent. In the present work, the typical scale of the problem is a few m_c , but in [31], the numerical parameters are given for $\mu = m_c$ and $\mu = \infty$. In the present work, the values of the numerical parameters at the scale $\mu = m_c$ are used. Changing the scale to $\mu = \infty$ modified the obtained results by less than 3%.

Another ingredient to obtain the numerical values of the right hand side of eq. (41) are the Borel parameter M^2 and the continuum threshold, s_0 . The Borel parameter, M^2 , is an auxiliary parameter and physical quantities like the form factor should be independent of its value. Due to the approximations used in the method, a residual M^2 dependence might remain. To reduce this dependence, a suitable region of M^2 should be chosen such that the predictions are independent of this parameter [37–46]. On the other hand, the threshold parameter, s_0 , is mainly related to hadron mass in question. It is usually chosen as $s_0 \simeq (m_{hadron} \pm 0.5 \text{ GeV})^2$. The upper limit of the M^2 region can be determined by requiring the contribution of the lowest pole to be at least 50%, whereas the lower limit can be determined by requiring the convergence of the twist expansion. In fig. 2, the relative contribution of the subleading twist distribution amplitudes to the final result for the form factors f_1 and f_{V+} are shown as two examples. As can be seen in the figure, the relative contribution of the subleading twist distribution amplitudes diminish rapidly with increasing M^2 for the form factor f_1 , but for f_{V+} the reduction rate is smaller. For $M^2 > 5 \text{ GeV}^2$, the contribution of the subleading twist terms to all the form factors are found to be less than 15%. Note that this is true, even though the subleading DAs are enhanced by the heavy meson mass.

To analyse the pole contribution, the following ratio is studied [45]:

$$Pole = \frac{\int_0^{s_0} ds \rho^{QCD}(s) e^{-\frac{s}{M^2}}}{\int_0^\infty ds \rho^{QCD}(s) e^{-\frac{s}{M^2}}}. \quad (46)$$

The pole contribution to the form factor is shown in fig. 3. As can be seen from this figure, the pole contribution is more than 50% if $M^2 < 10 \text{ GeV}^2$. It is found that this is also correct for all the form factors. Note that, in analysis, once the Borel region is determined, it is expected that the physical parameters are independent of the Borel parameter within this

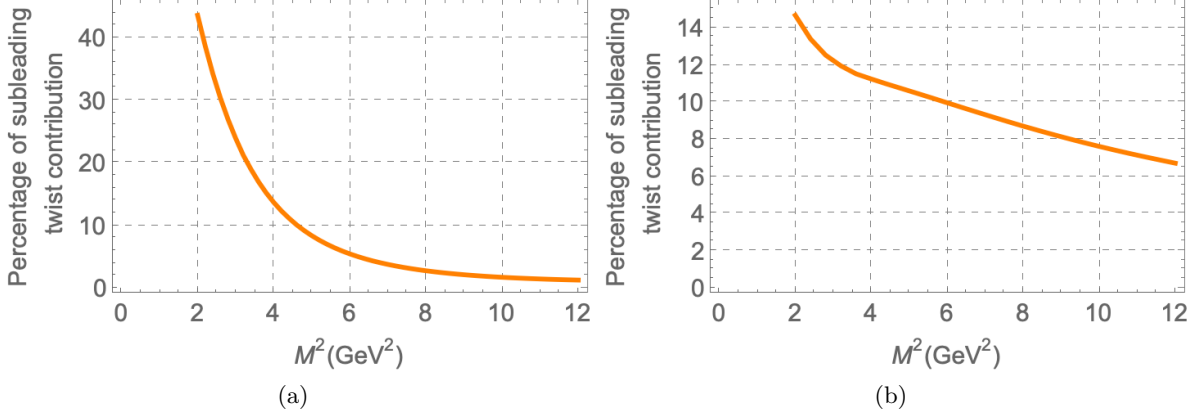


Figure 2: The percentage of subleading twist contribution- M^2 plot for $s_0 = 40 \text{ GeV}^2$ and $q^2 = 0 \text{ GeV}^2$. (a) For f_1 form factor of 1^3P_0 charmonium. (b) For f_{V+} form factor of 1^3P_1 charmonium.

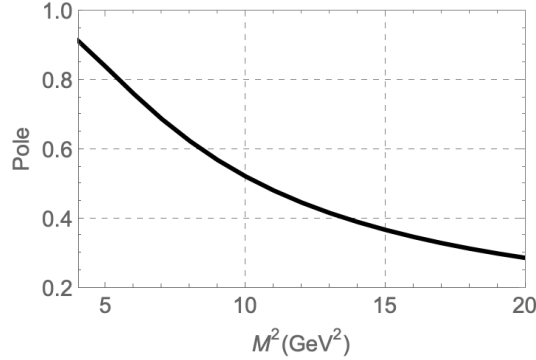


Figure 3: *Pole- M^2* plot of 1^3P_2 state's f_{T_0} form factor for $q^2 = 0 \text{ GeV}^2$ and $s_0 = 40 \text{ GeV}^2$.

region. As an example, in fig. 4, the M^2 dependence of the form factor $f_{T_0}(q^2)$ for 1^3P_2 state is shown for various s_0 and q^2 values. It is seen in this figure that for the chosen s_0 values, the prediction on the form factor is practically independent of the value of M^2 within the determined region. The same conclusion also holds for other form factors. Hence, in further analysis, all the form factors will be analysed in the Borel region $5 \text{ GeV}^2 < M^2 < 10 \text{ GeV}^2$ for the s_0 values $s_0 = 40 \pm 5 \text{ GeV}^2$.

Using the parameters discussed above, numerical values of the right hand side of the sum rules given in eq. (41) can be obtained. To predict numerical values of the form factors, it is necessary to choose a value for the mass of the B_c meson. Frequently, the value of the hadron in question is picked from the experiment, if it is experimentally known. But this assumes that eq. (41) predicts the mass of the hadron precisely. In order to avoid this assumption, the mass of the B_c meson will also be obtained from eq. (41) using the relation

$$m_{B_c}^2 = \frac{\int_0^{s_0} ds s \rho^{QCD}(q^2, s) e^{-\frac{s}{M^2}}}{\int_0^{s_0} ds \rho^{QCD}(q^2, s) e^{-\frac{s}{M^2}}} \quad (47)$$

The masses obtained using eq. (47) should be stable with respect to variations of M^2 in chosen

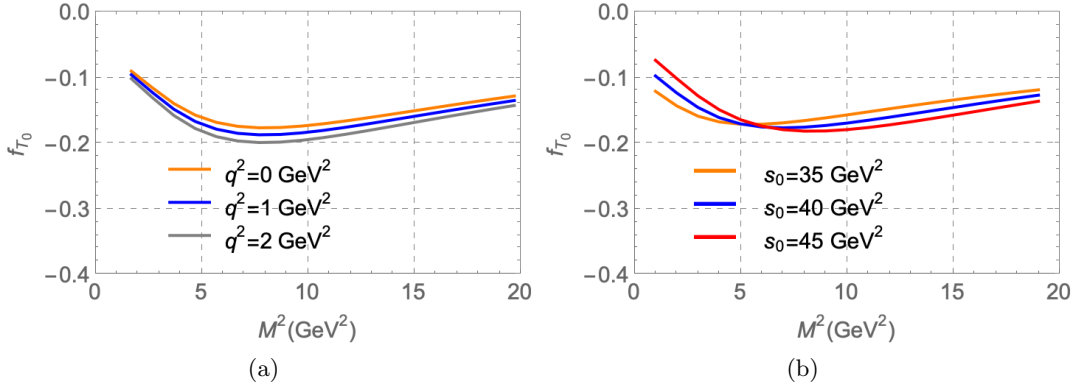


Figure 4: (a) 1^3P_2 state's f_{T_0} form factor with respect to M^2 for $s_0 = 40 \text{ GeV}^2$ and $q^2 = 0 \text{ GeV}^2$ (blue line), 1 GeV^2 (orange line), and 2 GeV^2 (gray line). (b) 1^3P_2 state's f_{T_0} form factor with respect to M^2 for $q^2 = 0 \text{ GeV}^2$ and $s_0 = 35 \text{ GeV}^2$ (orange line), 40 GeV^2 (blue line), and 45 GeV^2 (red line).

region. In fig. 5, the dependence of m_{B_c} obtained from eq. (47) on the Borel parameter M^2 is presented for $s_0 = 40 \text{ GeV}^2$ using the sum rules for the form factor $f_1(0)$. As can be seen in this figure, the mass is practically independent of the borel parameter M^2 in the chosen region. For comparison, in fig. 6, the Borel parameter dependence of f_1 is shown when eq. (47) is used for $m_{B_c}^2$ and when its experimental value is used. It is clearly seen that the form factors has a stronger dependence on the Borel parameter when the experimental value is used. This shows that after the continuum and higher states are subtracted, the correlation function does have the form given in the left hand side of eq. (41) but the exponent predicted by the correlation function deviates from the experimentally observed mass. This is an expected behaviour as the obtained correlation function is only approximate and we strongly believe the correct procedure should be to use the mass of B_c which is predicted by the calculated correlation function.

In table 2, the working region of the Borel parameter and the B_c mass obtained from the corresponding sum rules is shown for each of the form factors. As can be noted from the table, the predicted masses for B_c are in general lower than the experimentally observed value. Note that this is not a consequence of the approach used in this work. When the sum rules for the form factors obtained in [27] is analyzed using the approach presented in this work, the obtained masses are compatible with the ones presented in table 2.

In the semileptonic decays of B_c mesons, the relevant q^2 values do not always lie in the region where the sum rules predictions are reliable. For this reason, the form factors obtained using QCD sum rules in the region of q^2 where the sum rules' predictions are reliable needs to be extrapolated to whole of the physically relevant region.

For the extrapolation, a suitable chosen extrapolation function is used. The explicit form of this function is another source of error in the predictions that depend the values of the form factors in the whole kinematical region. To estimate this additional error, the following two commonly used functions are used to extrapolate the form factors to the whole kinematical

Charmonia	Form Factor	State	$m_{B_c} (GeV)$
3P_0	f_1^n	$n = 1$	5.67 ± 0.02
		$n = 2$	5.59 ± 0.01
		$n = 3$	5.38 ± 0.01
	f_2^n	$n = 1$	5.72 ± 0.01
		$n = 2$	5.59 ± 0.02
		$n = 3$	5.37 ± 0.01
1P_1	f_V^n	$n = 1$	5.88 ± 0.05
		$n = 2$	5.86 ± 0.05
		$n = 3$	5.71 ± 0.08
	f_{V+}^n	$n = 1$	5.45 ± 0.05
		$n = 2$	5.54 ± 0.05
		$n = 3$	5.54 ± 0.15
	f_{V-}^n	$n = 1$	5.82 ± 0.05
		$n = 2$	5.73 ± 0.05
		$n = 3$	5.59 ± 0.15
	f_{V0}^n	$n = 1$	5.20 ± 0.05
		$n = 2$	5.11 ± 0.04
		$n = 3$	5.10 ± 0.04
3P_1	f_V^n	$n = 1$	5.80 ± 0.12
		$n = 2$	5.72 ± 0.12
		$n = 3$	5.54 ± 0.12
	f_{V+}^n	$n = 1$	5.47 ± 0.15
		$n = 2$	5.47 ± 0.12
		$n = 3$	5.37 ± 0.12
	f_{V-}^n	$n = 1$	5.28 ± 0.05
		$n = 2$	5.51 ± 0.05
		$n = 3$	5.40 ± 0.02
	f_{V0}^n	$n = 1$	4.45 ± 0.02
		$n = 2$	4.05 ± 0.10
		$n = 3$	4.72 ± 0.02
3P_2	f_T^n	$n = 1$	5.22 ± 0.12
		$n = 2$	5.19 ± 0.10
		$n = 3$	5.14 ± 0.10
	f_{T+}^n	$n = 1$	4.58 ± 0.15
		$n = 2$	4.60 ± 0.08
		$n = 3$	4.57 ± 0.08
	f_{T-}^n	$n = 1$	4.58 ± 0.15
		$n = 2$	4.60 ± 0.08
		$n = 3$	4.57 ± 0.08
	f_{T0}^n	$n = 1$	4.88 ± 0.09
		$n = 2$	4.87 ± 0.09
		$n = 3$	4.24 ± 0.07

Table 2: Mass prediction of B_c meson from all form factors in $5 \text{ GeV}^2 \leq M^2 \leq 10 \text{ GeV}^2$. Here the error comes from s_0 region ($35 \text{ GeV}^2 \leq s_0 \leq 45 \text{ GeV}^2$).

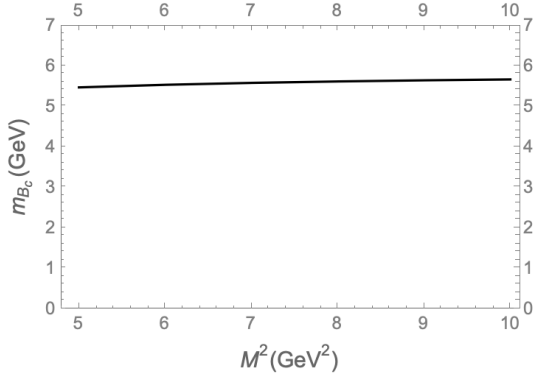


Figure 5: m_{B_c} - M^2 plot (where m_{B_c} is computed from 1^3P_0 state's f_1 form factor) for $q^2 = 0 \text{ GeV}^2$ and $s_0 = 40 \text{ GeV}^2$.

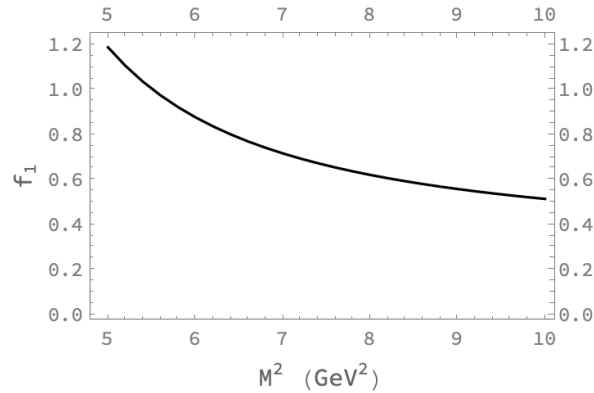


Figure 6: 1^3P_0 state's f_1 form factor with respect to M^2 for experimentally measured B_c mass (6.28 GeV) for $q^2 = 0$ and $s_0 = 40 \text{ GeV}^2$.

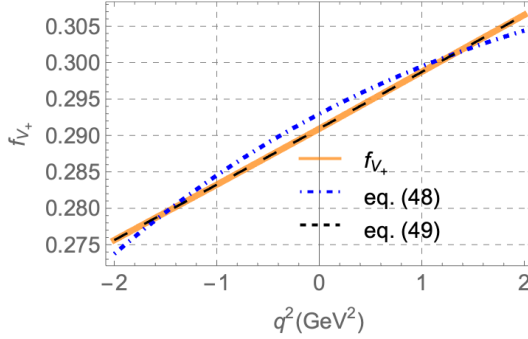


Figure 7: f_{V+} - q^2 plot of 1^1P_1 axial-vector meson and its fit functions.

q^2 region.

$$f_i^n(q^2) = \frac{a}{\left(1 - \frac{q^2}{m_{fit}^2}\right)} + \frac{b}{\left(1 - \frac{q^2}{m_{fit}^2}\right)^2}, \quad (48)$$

$$f_i^n(q^2) = F_0 \exp\left\{a\left(\frac{q^2}{m_{fit}^2}\right) + b\left(\frac{q^2}{m_{fit}^2}\right)^2\right\}, \quad (49)$$

where F_0 , a , b , and m_{fit} are the fit parameters. These parameters are chosen so that this function overlaps with the form factor prediction obtained in the region of q^2 where the predictions are reliable. The obtained values are shown in appendix B. In eq. (48), the fit parameter m_{fit} obtained from the fit to various form factors all turned out to be very close to $m_{fit} = 5.18 \text{ GeV}$. Hence, we fixed this parameter at this value for the fits. In the region $-2 \text{ GeV}^2 < q^2 < 2 \text{ GeV}^2$, the two fit functions reliably reproduce the obtained predictions. The largest difference between the best fits obtained for the two different fit functions is observed in f_{V+} for 1^1P_1 charmonium. In fig. 7 this form factors along with the fits obtained by the two functions are shown. As can be seen from this figure, even the largest difference between the two functions is less than 1%.

4 Semileptonic Decay Rates

Once the formfactors are obtained, they can be used to analyze the semileptonic decay rates of the B_c meson into P-wave charmonia. The decay rates can be expressed in terms of helicity amplitudes as [33–36]:

$$\frac{d\Gamma(B_c \rightarrow c\bar{c}l\bar{\nu})}{dq^2} = \frac{G_F^2}{(2\pi)^3} |V_{bc}|^2 \frac{\lambda^{1/2}(q^2 - m_l^2)^2}{24 m_{B_c}^3 q^2} \left[HH^\dagger \left(1 + \frac{m_l^2}{2q^2}\right) + \frac{3m_l^2}{2q^2} H_t H_t^\dagger \right] \quad (50)$$

where $\lambda = m_{B_c}^4 + m_{c\bar{c}}^4 + q^4 - 2(m_{B_c}^2 m_{c\bar{c}}^2 + m_{c\bar{c}}^2 q^2 + m_{B_c}^2 q^2)$, $m_{B_c} = 6.28 \text{ GeV}$, $m_{c\bar{c}}$ is the corresponding charmonium mass (m_S , m_A , m_T) and m_l is the corresponding lepton mass ($m_e = 0.5 \text{ MeV}$, $m_\mu = 105.66 \text{ MeV}$, $m_\tau = 1.78 \text{ GeV}$) and

$$HH^\dagger \equiv H_+ H_+^\dagger + H_- H_-^\dagger + H_0 H_0^\dagger \quad (51)$$

where the subscripts \pm , 0 , t denote transverse, longitudinal and time like helicity components, respectively and they are defined in terms of the form factors as

- Spin 0: $B_c \rightarrow S(^3P_0)$ transition

$$\begin{aligned} H_{\pm} &= 0, \\ H_0 &= \frac{\lambda^{1/2}}{\sqrt{q^2}} f_1^n(q^2), \\ H_t &= \frac{1}{\sqrt{q^2}} [(m_{B_c}^2 - m_S^2) f_1^n(q^2) + q^2 f_2^n(q^2)] \end{aligned} \quad (52)$$

where m_S is the scalar meson mass.

- Spin 1: $B_c \rightarrow A(^3P_1, ^1P_1)$ transition

$$\begin{aligned} H_{\pm} &= -(m_{B_c} + m_A) f_{V_0}^n(q^2) \mp \frac{\lambda^{1/2}}{m_{B_c} + m_A} f_V^n(q^2), \\ H_0 &= \frac{1}{2m_A \sqrt{q^2}} \left\{ -(m_{B_c}^2 - m_A^2 - q^2)(m_{B_c} + m_A) f_{V_0}^n(q^2) + \frac{\lambda^{1/2}}{m_{B_c} + m_A} f_{V_+}^n(q^2) \right\}, \\ H_t &= \frac{\lambda^{1/2}}{2m_A \sqrt{q^2}} \left\{ -(m_{B_c} + m_A) f_{V_0}^n(q^2) + (m_{B_c} - m_A) f_{V_+}^n(q^2) + \frac{q^2}{m_{B_c} + m_A} f_{V_-}^n(q^2) \right\}. \end{aligned} \quad (53)$$

Notice that $f_{V_+}^n$, $f_{V_-}^n$, $f_{V_0}^n$, and $f_{V_0}^n$ form factors for the 1P_1 charmonium state and $f_{V_+}^n$, $f_{V_-}^n$, $f_{V_0}^n$, and $f_{V_0}^n$ form factors for the 3P_1 charmonium state are simplified as f_V^n , $f_{V_+}^n$, $f_{V_-}^n$, and $f_{V_0}^n$.

- Spin 2: $B_c \rightarrow T(^3P_2)$ transition

$$\begin{aligned} H_{\pm} &= \frac{\lambda^{1/2}}{2\sqrt{2}m_{B_c}m_T} \left\{ (m_{B_c} + m_T) f_{T_0}^n(q^2) \pm \frac{\lambda^{1/2}}{m_{B_c} + m_T} f_T^n(q^2) \right\}, \\ H_0 &= \frac{\lambda^{1/2}}{2\sqrt{6}m_{B_c}m_T} \left\{ (m_{B_c} + m_T)(m_{B_c}^2 - m_T^2 - q^2) f_{T_0}^n(q^2) - \frac{\lambda}{m_{B_c}} f_{T_+}^n(q^2) \right\}, \\ H_t &= \sqrt{\frac{2}{3}} \frac{\lambda}{4m_{B_c}m_T^2 \sqrt{q^2}} \left\{ (m_{B_c} + m_T) f_{T_0}^n(q^2) - \frac{m_{B_c}^2 - m_T^2}{m_{B_c}} f_{T_+}^n(q^2) - \frac{q^2}{m_{B_c}} f_{T_-}^n(q^2) \right\}. \end{aligned} \quad (54)$$

where m_S , m_{AV} , and m_T are the corresponding charmonium mass and they are given in table 1. The physical region for q^2 is defined as $m_l^2 \leq q^2 \leq (m_{B_c} - m_{c\bar{c}})^2$. In figs. 8 to 11 the differential B_c decay rates are shown for various final states. In these figures, the fit function in eq. (48) is used. As can be seen from the figures, the differential decay rates for decays involving e and μ are almost identical, whereas the differential decay rate for decays involving τ is significantly lower due to τ 's heavy mass.

Finally, we present branching ratios for each ground state and excited states of P-wave charmonia and compare them with the results in the literature in table 3. As can be seen from the table, the choice of the fit function does not influence the branching ratios for decays into scalar and tensor charmonia, whereas the branching ratios for the decays into axial vector charmonia change by upto a factor two. As is mentioned in the introduction, there are no QCDSR predictions for decays into final states containing excited P-wave charmonia. The presented results from literature are obtained using non-relativistic quark model computations. As can be seen from the tables, our predictions for decays into final states 1P_0

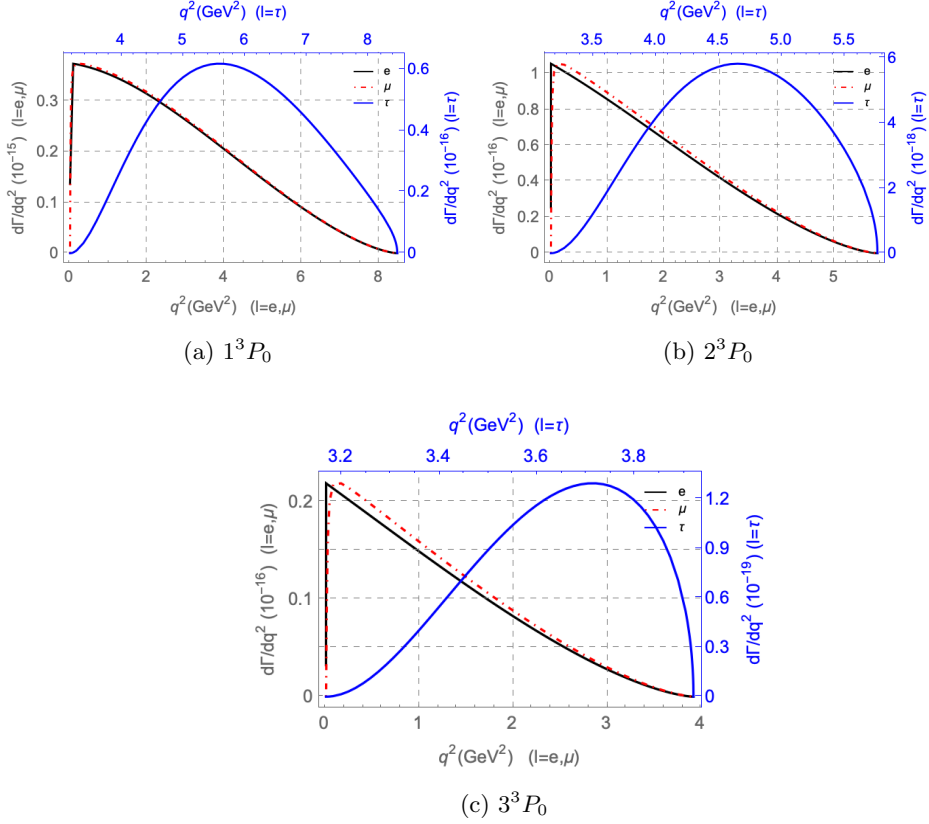


Figure 8: $d\Gamma/dq^2$ - q^2 plots for decays involving 3P_0 scalar meson and its excited states for e , μ , and τ leptons in the final states. There are two different scales for q^2 and $d\Gamma/dq^2$ in each frame since left and bottom axis of frame are for e and μ leptons and right and up axis of frame are for τ lepton.

and 1P_1 are within the range of other predictions in the literature, where as for the final state 3P_2 , our predictions are slightly smaller, and for the final state 3P_1 our prediction is slightly larger than the existing predictions in the literature. As our predictions for decays not involving radially excited charmonia are compatible with the existing results in the literature, this can be taken as an indication that the results for the excited state are also reliable. It should also be noted that, keeping only the form factors f_1 , f_{V_0} and f_{T_0} and setting all the other form factors to zero, the changes in the branching ratios are less than 10%.

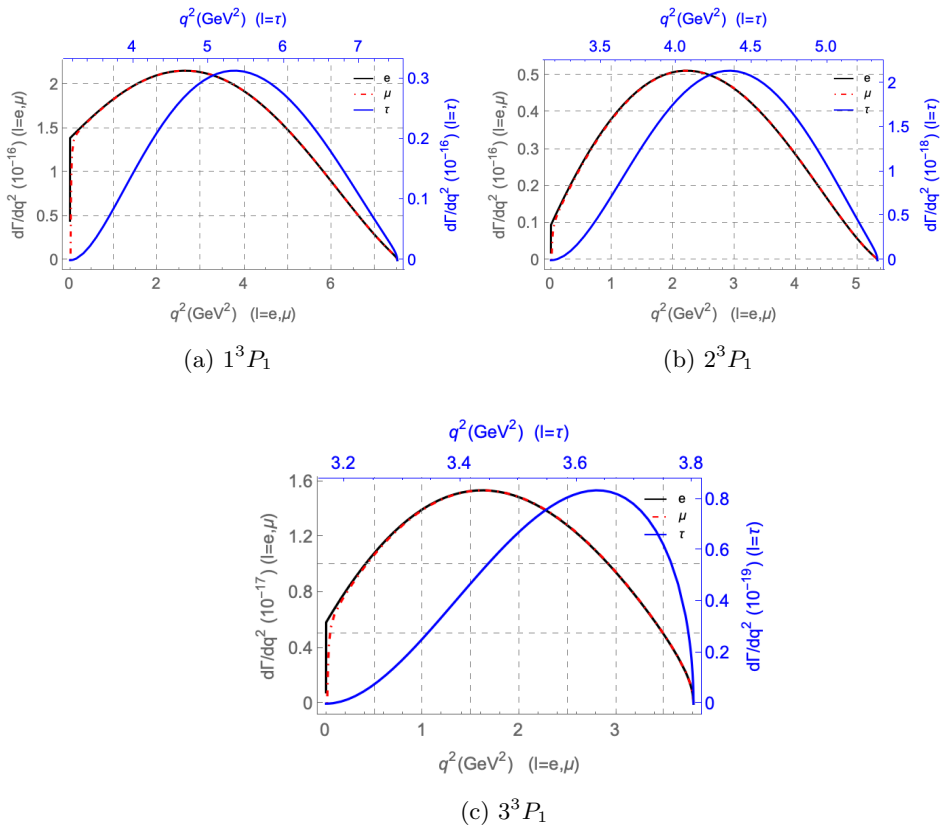


Figure 9: $d\Gamma/dq^2$ - q^2 plots for decays involving 3P_1 scalar meson and its excited states for e , μ , and τ leptons

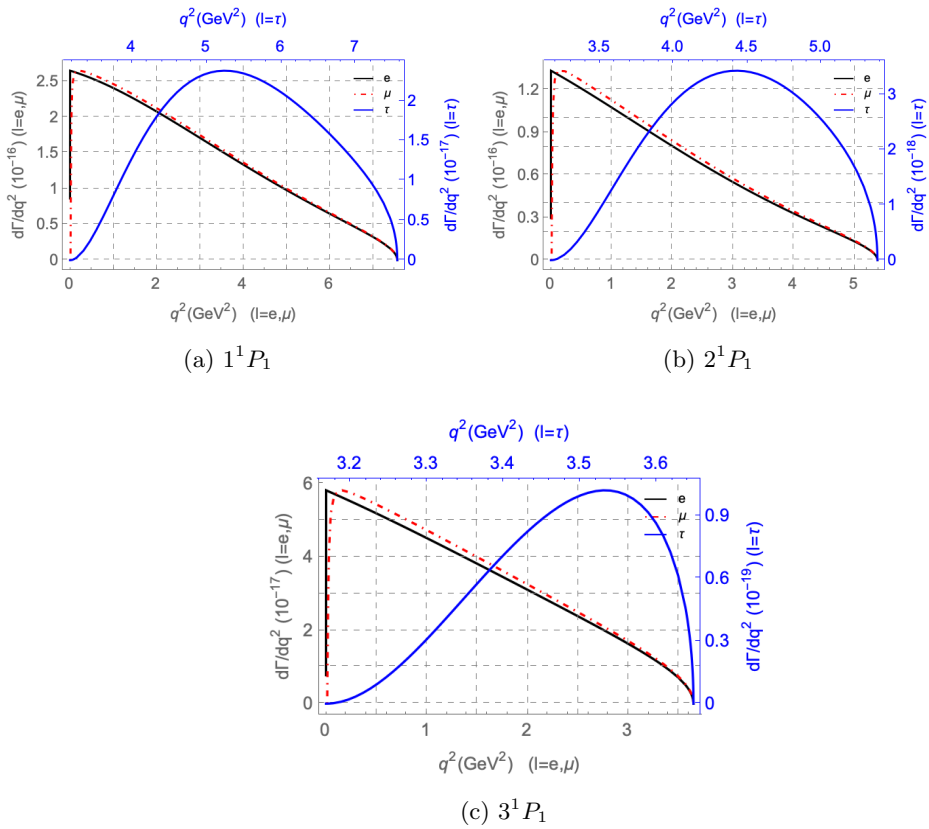


Figure 10: $d\Gamma/dq^2$ - q^2 plots for decays involving 1P_1 scalar meson and its excited states for e , μ , and τ leptons

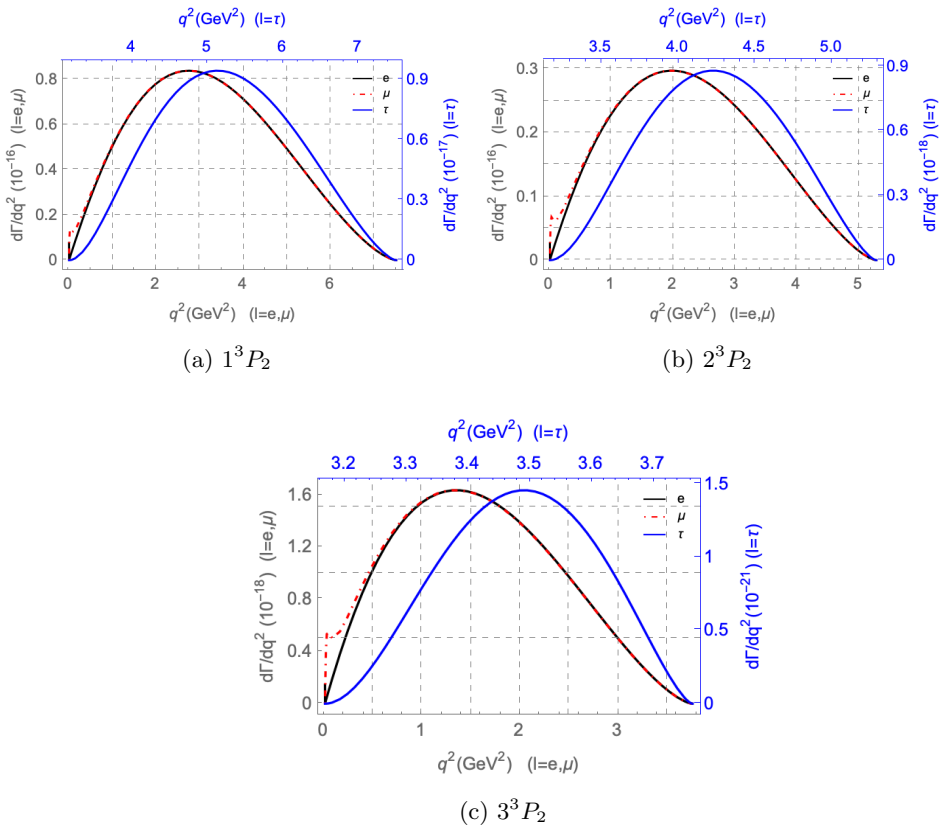


Figure 11: $d\Gamma/dq^2$ - q^2 plots for decays involving 3P_2 scalar meson and its excited states for e , μ , and τ leptons

$c\bar{c}$	This paper	[27] QCDSR	[33] RQMQP	[54] RQM	[49] NRQM	This paper	[27] QCDSR	[33] RQMQP	[54] RQM	[49] NRQM
	$l = e, \mu$	$l = e$	$l = e$	$l = e$	$l = e$	$l = \tau$	$l = \tau$	$l = \tau$	$l = \tau$	$l = \tau$
1^3P_0	0.114 (0.119)	0.182	0.087	0.180	0.110	0.0014 (0.0017)	0.018	0.0075	0.018	0.013
2^3P_0	0.020 (0.019)	—	0.014	—	—	6.8×10^{-4} (6.0×10^{-4})	—	6.3×10^{-4}	—	—
3^3P_0	0.0027 (0.0024)	—	—	—	—	4.04×10^{-6} (2.73×10^{-6})	—	—	—	—
1^1P_1	0.077 (0.108)	0.142	0.096	0.310	0.170	0.0048 (0.0104)	0.0137	0.0077	0.027	0.015
2^1P_1	0.026 (0.025)	—	0.0021	—	—	3.5×10^{-4} (5.6×10^{-4})	—	0.00011	—	—
3^1P_1	0.0089 (0.0124)	—	—	—	—	1.97×10^{-6} (2.51×10^{-6})	—	—	—	—
1^3P_1	0.080 (0.112)	0.146	0.082	0.098	0.066	0.0057 (0.0079)	0.0147	0.0092	0.012	0.0072
2^3P_1	0.013 (0.022)	—	0.0085	—	—	1.9×10^{-4} (2.51×10^{-4})	—	3.9×10^{-4}	—	—
3^3P_1	0.003 (0.004)	—	—	—	—	2.16×10^{-6} (1.34×10^{-6})	—	—	—	—
1^3P_2	0.026 (0.025)	—	0.160	0.200	0.130	0.0019 (0.0018)	—	0.0093	0.014	0.0093
2^3P_2	0.0066 (0.0061)	—	0.0033	—	—	7.36×10^{-5} (7.0×10^{-5})	—	1.3×10^{-4}	—	—
3^3P_2	0.00023 (0.00023)	—	—	—	—	3.39×10^{-8} (2.47×10^{-8})	—	—	—	—

Table 3: Branching Ratios (in %) of semi-leptonic B_c decays to P-wave charmonia ($B_c \rightarrow (c\bar{c}) l \bar{\nu}$) for fixed value of the B_c lifetime $\tau_{B_c} = 0.46 \text{ ps}$. In the column showing our results the numbers in parenthesis are the results obtained for the exponential fit.

5 Conclusions

In this work, the form factors and differential decay rates of semileptonic decays of B_c meson into P-wave charmonia and their excited states in the framework of LCSR. The excited states are parameterized by distribution amplitudes obtained from non-relativistic QM wave functions in [31]. In the literature, there are studies of B_c decays into the P-wave charmonia in the ground states. For these states, the results obtained in this work and those available in the literature are comparable. This indicates that the approach used in this work of using QM wave functions to model the charmonium states are reliable. Hence, it is reasonable to assume that the obtained results for the excited states are also reliable.

Acknowledgments

This research has been supported by TUBITAK (The Scientific and Technological Research Council of Turkey) under the grant no 117F090. The authors would like to thank M. A. Olpak for his useful discussions.

A Formulae for form factors

The analytic results of the form factors are below

$$\begin{aligned}
f_1^n(q^2)\kappa_{f_1^n} e^{-\frac{m_{B_c}^2}{M^2}} &= \frac{3}{2} m_b f_S m_S^2 e^{-\frac{s_0}{M^2}} \int_0^1 du \int_0^u dt \frac{\phi_S(u) \delta(s_0 - s(t, q^2, m_S^2))}{t} \\
&+ \frac{3m_b f_S m_S^2}{2M^2} \int_0^{s_0} ds \int_0^1 du \int_0^u dt \frac{e^{-\frac{s}{M^2}} \phi_S(u) \delta(s - s(t, q^2, m_S^2))}{t} \\
&+ \frac{3}{4} m_b f_S m_S^2 e^{-\frac{s_0}{M^2}} \int_0^1 du \int_0^u dt \int_0^u dv \frac{\phi_S(v) \delta(s_0 - s(t, q^2, m_S^2))}{t(v-1)} \\
&- \frac{3}{4} m_b f_S m_S^2 e^{-\frac{s_0}{M^2}} \int_0^1 du \int_0^u dt \int_u^1 dv \frac{\phi_S(v) \delta(s_0 - s(t, q^2, m_S^2))}{tv} \\
&+ \frac{3m_b f_S m_S^2}{4M^2} \int_0^{s_0} ds \int_0^1 du \int_0^u dt \int_0^u dv \frac{e^{-\frac{s}{M^2}} \phi_S(v) \delta(s - s(t, q^2, m_S^2))}{t(v-1)} \\
&- \frac{3m_b f_S m_S^2}{4M^2} \int_0^{s_0} ds \int_0^1 du \int_0^u dt \int_u^1 dv \frac{e^{-\frac{s}{M^2}} \phi_S(v) \delta(s - s(t, q^2, m_S^2))}{tv} \\
&- \frac{3}{2} m_b f_S \int_0^{s_0} ds \int_0^1 du \frac{e^{-\frac{s}{M^2}} \phi_S(u) \delta(s - s(u, q^2, m_S^2))}{u}
\end{aligned} \tag{55}$$

where

$$s(u, q^2, m^2) = \bar{u}m^2 + \frac{m_b^2 - \bar{u}q^2}{u} \tag{56}$$

$$\begin{aligned}
f_2^n(q^2) \kappa_{f_2^n} e^{-\frac{m_{B_c}^2}{M^2}} = & -\frac{3}{2} m_b f_S m_S^2 e^{-\frac{s_0}{M^2}} \int_0^1 du \int_0^u dt \frac{(t-2) \phi_S(u) \delta(s_0 - s(t, q^2, m_S^2))}{t^2} \\
& -\frac{3 m_b f_S m_S^2}{2 M^2} \int_0^{s_0} ds \int_0^1 du \int_0^u dt \frac{(t-2) e^{-\frac{s}{M^2}} \phi_S(u) \delta(s - s(t, q^2, m_S^2))}{t^2} \\
& -\frac{3}{4} m_b f_S m_S^2 e^{-\frac{s_0}{M^2}} \int_0^1 du \int_0^u dt \int_0^u dv \frac{(t-2) \phi_S(v) \delta(s_0 - s(t, q^2, m_S^2))}{t^2(v-1)} \\
& +\frac{3}{4} m_b f_S m_S^2 e^{-\frac{s_0}{M^2}} \int_0^1 du \int_0^u dt \int_u^1 dv \frac{(t-2) \phi_S(v) \delta(s_0 - s(t, q^2, m_S^2))}{t^2 v} \\
& -\frac{3 m_b f_S m_S^2}{4 M^2} \int_0^{s_0} ds \int_0^1 du \int_0^u dt \int_0^u dv \frac{(t-2) e^{-\frac{s}{M^2}} \phi_S(v) \delta(s - s(t, q^2, m_S^2))}{t^2(v-1)} \\
& +\frac{3 m_b f_S m_S^2}{4 M^2} \int_0^{s_0} ds \int_0^1 du \int_0^u dt \int_u^1 dv \frac{(t-2) e^{-\frac{s}{M^2}} \phi_S(v) \delta(s - s(t, q^2, m_S^2))}{t^2 v} \\
& +\frac{3}{2} m_b f_S \int_0^{s_0} ds \int_0^1 du \frac{e^{-\frac{s}{M^2}} \phi_S(u) \delta(s - s(u, q^2, m_S^2))}{u}
\end{aligned} \tag{57}$$

$$f_V^n(q^2) \kappa_{f_V^n} e^{-\frac{m_{B_c}^2}{M^2}} = 3 f_{A_\perp} \int_0^{s_0} ds \int_0^1 du \frac{e^{-\frac{s}{M^2}} \phi_{A_\perp}(u) \delta(s - s(u, q^2, m_A^2))}{u} \tag{58}$$

$$\begin{aligned}
f_{V_0}^n(q^2) \kappa_{f_{V_0}^n} e^{-\frac{m_{B_C}^2}{M^2}} = & -\frac{3m_A^2}{2M^2} \int_0^{s_0} ds \int_0^1 du \int_0^u dt \frac{e^{-\frac{s}{M^2}} \delta(s - s(t, q^2, m_A^2))}{t^2} \\
& \times \left(2m_A f_{A_{||}} m_b (u - t) \phi_{A_{||}}(u) + f_{A_{\perp}} \phi_{A_{\perp}}(u) (2m_b^2 + M^2 t) \right) \\
& + 3m_A^2 m_b e^{-\frac{s_0}{M^2}} \int_0^1 du \int_0^u dt \frac{\delta(s_0 - s(t, q^2, m_A^2))}{t^2} \\
& \times \left(m_A f_{A_{||}} (t - u) \phi_{A_{||}}(u) - f_{A_{\perp}} m_b \phi_{A_{\perp}}(u) \right) \\
& + \frac{3m_A^2}{2M^2} \int_0^{s_0} ds \int_0^1 du \int_0^u dt \int_0^u dv \frac{e^{-\frac{s}{M^2}} \delta(s - s(t, q^2, m_A^2))}{t^2(v-1)} \\
& \times \left(m_A f_{A_{||}} m_b (t - u) \phi_{A_{||}}(v) + (2u - 1) f_{A_{\perp}} \phi_{A_{\perp}}(v) (2m_b^2 + M^2 t) \right) \\
& - \frac{3m_A^2}{2M^2} \int_0^{s_0} ds \int_u^1 du \int_0^1 dt \int_0^u dv \frac{e^{-\frac{s}{M^2}} \delta(s - s(t, q^2, m_A^2))}{t^2 v} \\
& \times \left(m_A f_{A_{||}} m_b (t - u) \phi_{A_{||}}(v) + (2u - 1) f_{A_{\perp}} \phi_{A_{\perp}}(v) (2m_b^2 + M^2 t) \right) \\
& + \frac{3}{2} m_A^2 m_b e^{-\frac{s_0}{M^2}} \int_0^1 du \int_0^u dt \int_u^1 dv \frac{\delta(s_0 - s(t, q^2, m_A^2))}{t^2 v} \\
& \times \left(m_A f_{A_{||}} (u - t) \phi_{A_{||}}(v) + 2(1 - 2u) f_{A_{\perp}} m_b \phi_{A_{\perp}}(v) \right) \\
& + \frac{3}{2} m_A^2 m_b e^{-\frac{s_0}{M^2}} \int_0^1 du \int_0^u dt \int_0^u dv \frac{\delta(s_0 - s(t, q^2, m_A^2))}{t^2(v-1)} \\
& \times \left(m_A f_{A_{||}} (t - u) \phi_{A_{||}}(v) + 2(2u - 1) f_{A_{\perp}} m_b \phi_{A_{\perp}}(v) \right) \\
& + \frac{3}{2} m_A f_{A_{||}} m_b \int_0^{s_0} ds \int_0^1 du \int_u^1 dv \frac{e^{-\frac{s}{M^2}} \phi_{A_{||}}(v) \delta(s - s(u, q^2, m_A^2))}{uv} \\
& + 3m_A f_{A_{||}} m_b \int_0^{s_0} ds \int_0^1 du \int_0^u dv \frac{e^{-\frac{s}{M^2}} \phi_{A_{||}}(v) \delta(s - s(u, q^2, m_A^2))}{2u - 2uv} \\
& + \frac{3}{2} f_{A_{\perp}} \int_0^{s_0} ds \int_0^1 du \frac{e^{-\frac{s}{M^2}} \phi_{A_{\perp}}(u) (u^2 m_A^2 + m_b^2 + q^2) \delta(s - s(u, q^2, m_A^2))}{u^2}
\end{aligned} \tag{59}$$

$$\begin{aligned}
f_{V_+}^n(q^2) \kappa_{f_{V_+}^n} e^{-\frac{m_{B_c}^2}{M^2}} &= \frac{3f_{A_\perp}}{2} \int_0^{s_0} ds \int_0^1 du \frac{e^{-\frac{s}{M^2}} \delta(s - s(u, q^2, m_A^2)) \phi_{A_\perp}(u)}{u} \\
&+ \frac{3m_A e^{-\frac{s_0}{M^2}}}{2M^2} \int_0^1 du \int_0^u dt \frac{\delta(s_0 - s(t, q^2, m_A^2))}{t^2} \\
&\times \left(t f_{A_\perp} m_A \phi_{A_\perp}(u) M^2 + 2 f_{A_\parallel} (M^2 + (t-u)m_A^2) m_b \phi_{A_\parallel}(u) \right) \\
&+ \frac{3m_A}{2M^4} \int_0^{s_0} ds \int_0^1 du \int_0^u dt \frac{e^{-\frac{s}{M^2}} \delta(s - s(t, q^2, m_A^2))}{t^2} \\
&\times \left(t f_{A_\perp} m_A \phi_{A_\perp}(u) M^2 + 2 f_{A_\parallel} (M^2 + (t-u)m_A^2) m_b \phi_{A_\parallel}(u) \right) \\
&+ \frac{3e^{-\frac{s_0}{M^2}} m_A}{2M^2} \int_0^1 du \int_0^u dt \int_0^u dv \frac{\delta(s_0 - s(t, q^2, m_A^2))}{t^2(v-1)} \\
&\times \left(t(1-2u) f_{A_\perp} m_A \phi_{A_\perp}(v) M^2 + f_{A_\parallel} (M^2 + (t-u)m_A^2) m_b \phi_{A_\parallel}(v) \right) \\
&- \frac{3e^{-\frac{s_0}{M^2}} m_A}{2M^2} \int_0^1 du \int_0^u dt \int_u^1 dv \frac{\delta(s_0 - s(t, q^2, m_A^2))}{t^2 v} \\
&\times \left(t(1-2u) f_{A_\perp} m_A \phi_{A_\perp}(v) M^2 + f_{A_\parallel} (M^2 + (t-u)m_A^2) m_b \phi_{A_\parallel}(v) \right) \\
&+ \frac{3m_A}{2M^4} \int_0^{s_0} ds \int_0^u du \int_0^1 dt \int_0^u dv \frac{e^{-\frac{s}{M^2}} \delta(s - s(t, q^2, m_A^2))}{t^2(v-1)} \\
&\times \left(t(1-2u) f_{A_\perp} m_A \phi_{A_\perp}(v) M^2 + f_{A_\parallel} (M^2 + (t-u)m_A^2) m_b \phi_{A_\parallel}(v) \right) \\
&- \frac{3m_A}{2M^4} \int_0^{s_0} ds \int_0^1 du \int_0^u dt \int_u^1 dv \frac{e^{-\frac{s}{M^2}} \delta(s - s(t, q^2, m_A^2))}{t^2 v} \\
&\times \left(t(1-2u) f_{A_\perp} m_A \phi_{A_\perp}(v) M^2 + f_{A_\parallel} (M^2 + (t-u)m_A^2) m_b \phi_{A_\parallel}(v) \right) \\
&+ 3f_{A_\parallel} m_b m_A^3 \frac{\partial}{\partial s_0} e^{-\frac{s_0}{M^2}} \int_0^1 du \int_0^u dt \frac{(t-u)\delta(s_0 - s(t, q^2, m_A^2)) \phi_{A_\parallel}(u)}{t^2} \\
&+ \frac{3f_{A_\parallel} m_b m_A^3}{2} \frac{\partial}{\partial s_0} e^{-\frac{s_0}{M^2}} \int_0^1 du \int_0^u dt \int_0^u dv \frac{(t-u)\delta(s_0 - s(t, q^2, m_A^2)) \phi_{A_\parallel}(v)}{t^2(v-1)} \\
&+ \frac{3f_{A_\parallel} m_b m_A^3}{2} \frac{\partial}{\partial s_0} e^{-\frac{s_0}{M^2}} \int_0^1 du \int_0^u dt \int_u^1 dv \frac{(u-t)\delta(s_0 - s(t, q^2, m_A^2)) \phi_{A_\parallel}(v)}{t^2 v}
\end{aligned} \tag{60}$$

$$\begin{aligned}
f_{V_-}^n(q^2) \kappa_{f_{V_-}^n} e^{-\frac{m_{B_c}^2}{M^2}} = & -\frac{3f_{A_\perp}}{2} \int_0^{s_0} ds \int_0^1 du \frac{e^{-\frac{s}{M^2}} \delta(s - s(u, q^2, m_A^2)) \phi_{A_\perp}(u)}{u} \\
& - \frac{3e^{-\frac{s_0}{M^2}} m_A}{2M^2} \int_0^1 du \int_0^u dt \frac{\delta(s_0 - s(t, q^2, m_A^2))}{t^3} \\
& \times \left((t-2) t f_{A_\perp} m_A \phi_{A_\perp}(u) M^2 + 2 f_{A_\parallel} (tM^2 + (t-2)(t-u)m_A^2) m_b \phi_{A_\parallel}(u) \right) \\
& - \frac{3m_A}{2M^4} \int_0^{s_0} ds \int_0^1 du \int_0^u dt \frac{e^{-\frac{s}{M^2}} \delta(s - s(t, q^2, m_A^2))}{t^3} \\
& \times \left((t-2) t f_{A_\perp} m_A \phi_{A_\perp}(u) M^2 + 2 f_{A_\parallel} (tM^2 + (t-2)(t-u)m_A^2) m_b \phi_{A_\parallel}(u) \right) \\
& - \frac{3e^{-\frac{s_0}{M^2}} m_A}{2M^2} \int_0^1 du \int_0^u dt \int_0^u dv \frac{\delta(s_0 - s(t, q^2, m_A^2))}{t^3(v-1)} \\
& \times \left(t(-2ut + t + 4u - 2) f_{A_\perp} m_A \phi_{A_\perp}(v) M^2 \right. \\
& \quad \left. + f_{A_\parallel} (tM^2 + (t-2)(t-u)m_A^2) m_b \phi_{A_\parallel}(v) \right) \\
& + \frac{3e^{-\frac{s_0}{M^2}} m_A}{2M^2} \int_0^1 du \int_0^u dt \int_u^1 dv \frac{\delta(s_0 - s(t, q^2, m_A^2))}{t^3 v} \\
& \times \left(t(-2ut + t + 4u - 2) f_{A_\perp} m_A \phi_{A_\perp}(v) M^2 \right. \\
& \quad \left. + f_{A_\parallel} (tM^2 + (t-2)(t-u)m_A^2) m_b \phi_{A_\parallel}(v) \right) \\
& - \frac{3m_A}{2M^4} \int_0^{s_0} ds \int_0^1 du \int_0^u dt \int_0^u dv \frac{e^{-\frac{s}{M^2}} \delta(s - s(t, q^2, m_A^2))}{t^3(v-1)} \\
& \times \left(t(-2ut + t + 4u - 2) f_{A_\perp} m_A \phi_{A_\perp}(v) M^2 \right. \\
& \quad \left. + f_{A_\parallel} (tM^2 + (t-2)(t-u)m_A^2) m_b \phi_{A_\parallel}(v) \right) \\
& + \frac{3m_A}{2M^4} \int_0^{s_0} ds \int_0^1 du \int_0^u dt \int_u^1 dv \frac{e^{-\frac{s}{M^2}} \delta(s - s(t, q^2, m_A^2))}{t^3 v} \\
& \times \left(t(-2ut + t + 4u - 2) f_{A_\perp} m_A \phi_{A_\perp}(v) M^2 \right. \\
& \quad \left. + f_{A_\parallel} (tM^2 + (t-2)(t-u)m_A^2) m_b \phi_{A_\parallel}(v) \right) \\
& + -3f_{A_\parallel} m_b m_A^3 \frac{\partial}{\partial s_0} e^{-\frac{s_0}{M^2}} \int_0^1 du \int_0^u dt \frac{(t-2)(t-u)\delta(s_0 - s(t, q^2, m_A^2)) \phi_{A_\parallel}(u)}{t^3} \\
& - \frac{3f_{A_\parallel} m_b m_A^3}{2} \frac{\partial}{\partial s_0} e^{-\frac{s_0}{M^2}} \int_0^1 du \int_0^u dt \int_0^u dv \frac{(t-2)(t-u)\delta(s_0 - s(t, q^2, m_A^2)) \phi_{A_\parallel}(v)}{t^3(v-1)} \\
& + \frac{3f_{A_\parallel} m_b m_A^3}{2} \frac{\partial}{\partial s_0} e^{-\frac{s_0}{M^2}} \int_0^1 du \int_0^u dt \int_u^1 dv \frac{(t-2)(t-u)\delta(s_0 - s(t, q^2, m_A^2)) \phi_{A_\parallel}(v)}{t^3 v}
\end{aligned} \tag{61}$$

$$f_T^n(q^2) \kappa_{f_T^n} e^{-\frac{m_{B_c}^2}{M^2}} = \frac{3}{2} f_{T_\perp}^n \int_0^1 du \int_0^u dt \frac{e^{-\frac{s_0}{M^2}} m_T \delta(s_0 - s(t; q^2, m_T^2)) \phi_{T_\perp}^n(u)}{t^2} \\ + \frac{3}{2} f_{T_\perp}^n \int_0^{s_0} ds e^{-\frac{s}{M^2}} \int_0^1 du \int_0^u dt \frac{m_T \delta(s - s(t; q^2, m_T^2)) \phi_{T_\perp}^n(u)}{M^2 t^2} \quad (62)$$

$$f_{T_0}^n(q^2) \kappa_{f_{T_0}^n} e^{-\frac{m_{B_c}^2}{M^2}} = \frac{3}{2} f_{T_\perp}^n \int_0^1 du \int_0^u dt \frac{e^{-\frac{s_0}{M^2}} m_T (m_b^2 + t^2 m_T^2 - q^2) \delta(s_0 - s(t; q^2, m_T^2)) \phi_{T_\perp}^n(u)}{t^3} \\ + \frac{3}{2} f_{T_\perp}^n \int_0^{s_0} ds e^{-\frac{s}{M^2}} \int_0^1 du \int_0^u dt \frac{m_T \delta(s - s(t; q^2, m_T^2))}{M^2 t^3} \\ \times (-t M^2 + m_b^2 + t^2 m_T^2 - q^2) \phi_{T_\perp}^n(u) \quad (63)$$

$$f_{T_+}^n(q^2) \kappa_{f_{T_+}^n} e^{-\frac{m_{B_c}^2}{M^2}} = -6 f_{T_\parallel}^n \frac{\partial}{\partial s_0} \int_0^1 du \int_0^u dt \frac{e^{-\frac{s_0}{M^2}} m_T^2 \delta(s_0 - s(t; q^2, m_T^2)) (t - u) m_b \phi_{T_\parallel}^n(u)}{t^3} \\ - 3 \int_0^1 du \int_0^u dt \frac{e^{-\frac{s_0}{M^2}} m_T^2 \delta(s_0 - s(t; q^2, m_T^2))}{M^2 t^3} \\ \times (t f_{T_\perp}^n \phi_{T_\perp}^n(u) M^2 + 2(t - u) f_{T_\parallel}^n m_b \phi_{T_\parallel}^n(u)) \\ - 6 \frac{\partial}{\partial s_0} \int_0^1 du \int_0^u dt \int_0^u dv \frac{e^{-\frac{s_0}{M^2}} (t - u) f_{T_\parallel}^n m_b m_T^2 \delta(s_0 - s(t; q^2, m_T^2)) \phi_{T_\parallel}^n(v)}{t^3 (v - 1)} \\ - 6 \int_0^1 du \int_0^u dt \int_0^u dv \frac{e^{-\frac{s_0}{M^2}} (t - u) f_{T_\parallel}^n m_b m_T^2 \delta(s_0 - s(t; q^2, m_T^2)) \phi_{T_\parallel}^n(v)}{M^2 t^3 (v - 1)} \\ + 6 \frac{\partial}{\partial s_0} \int_0^1 du \int_0^u dt \int_u^1 dv \frac{e^{-\frac{s_0}{M^2}} (t - u) f_{T_\parallel}^n m_b m_T^2 \delta(s_0 - s(t; q^2, m_T^2)) \phi_{T_\parallel}^n(v)}{t^3 v} \\ + 6 \int_0^1 du \int_0^u dt \int_u^1 dv \frac{e^{-\frac{s_0}{M^2}} (t - u) f_{T_\parallel}^n m_b m_T^2 \delta(s_0 - s(t; q^2, m_T^2)) \phi_{T_\parallel}^n(v)}{M^2 t^3 v} \\ - 3 \int_0^{s_0} ds e^{-\frac{s}{M^2}} \int_0^1 du \int_0^u dt \frac{m_T \delta(s - s(t; q^2, m_T^2))}{M^4 t^3} \\ \times (t f_{T_\perp}^n \phi_{T_\perp}^n(u) M^2 + 2(t - u) f_{T_\parallel}^n m_b m_T \phi_{T_\parallel}^n(u)) \\ - 6 \int_0^{s_0} ds e^{-\frac{s}{M^2}} \int_0^1 du \int_0^u dt \int_0^u dv \frac{(t - u) f_{T_\parallel}^n m_b m_T^2 \delta(s - s(t; q^2, m_T^2)) \phi_{T_\parallel}^n(v)}{M^4 t^3 (v - 1)} \\ + 6 \int_0^{s_0} ds \int_0^1 du \int_0^u dt \int_u^1 dv \frac{e^{-\frac{s}{M^2}} (t - u) f_{T_\parallel}^n m_T^2 \delta(s - s(t; q^2, m_T^2)) \phi_{T_\parallel}^n(v)}{M^4 t^3 v} \quad (64)$$

$$f_{T_-}^n = -f_{T_+}^n \quad (65)$$

B Fit Parameters

f_1^n				f_2^n			
State	a	b	$m_{fit} (GeV)$	State	a	b	$m_{fit} (GeV)$
$n = 1$	1.40	-1.07	5.18	$n = 1$	-1.55	1.18	5.18
$n = 2$	0.749	-0.528	5.18	$n = 2$	-0.757	0.533	5.18
$n = 3$	0.388	-0.260	5.18	$n = 3$	-0.378	0.253	5.18

Table 4: Fit parameters of f_1^n and f_2^n form factors for 3P_0 states in eq. (48).

f_V^n				f_{V+}^n			
State	a	b	$m_{fit} (GeV)$	State	a	b	$m_{fit} (GeV)$
$n = 1$	-1.39	1.14	5.18	$n = 1$	1.97	-1.56	5.18
$n = 2$	-1.22	0.967	5.18	$n = 2$	2.33	-1.80	5.18
$n = 3$	-1.52	1.12	5.18	$n = 3$	2.03	-1.55	5.18

f_{V-}^n				f_{V0}^n			
State	a	b	$m_{fit} (GeV)$	State	a	b	$m_{fit} (GeV)$
$n = 1$	-4.15	3.28	5.18	$n = 1$	-0.301	0.202	5.18
$n = 2$	-3.39	2.62	5.18	$n = 2$	-0.230	0.149	5.18
$n = 3$	-2.25	1.71	5.18	$n = 3$	-0.241	0.149	5.18

Table 5: Fit parameters of f_V^n , f_{V+}^n , f_{V-}^n , and f_{V0}^n form factors for 1P_1 states in eq. (48).

f_V^n				f_{V+}^n			
State	a	b	$m_{fit} (GeV)$	State	a	b	$m_{fit} (GeV)$
$n = 1$	4.85	-3.80	5.18	$n = 1$	-1.22	0.897	5.18
$n = 2$	3.67	-2.70	5.18	$n = 2$	-0.457	0.372	5.18
$n = 3$	2.15	-1.50	5.18	$n = 3$	-0.0843	0.110	5.18

f_{V-}^n				f_{V0}^n			
State	a	b	$m_{fit} (GeV)$	State	a	b	$m_{fit} (GeV)$
$n = 1$	0.852	-0.627	5.18	$n = 1$	0.211	-0.146	5.18
$n = 2$	0.492	-0.400	5.18	$n = 2$	0.0933	-0.0598	5.18
$n = 3$	0.0895	-0.116	5.18	$n = 3$	0.149	-0.0907	5.18

Table 6: Fit parameters of f_V^n , f_{V+}^n , f_{V-}^n , and f_{V0}^n form factors for 3P_1 states in eq. (48).

f_T^n			
State	a	b	$m_{fit} (GeV)$
$n = 1$	-0.765	0.646	5.18
$n = 2$	-0.856	0.698	5.18
$n = 3$	-0.721	0.573	5.18

$f_{T+}^n = -f_{T-}^n$			
State	a	b	$m_{fit} (GeV)$
$n = 1$	0.400	-0.320	5.18
$n = 2$	0.428	-0.334	5.18
$n = 3$	0.360	-0.274	5.18

$f_{T_0}^n$			
State	a	b	$m_{fit} (GeV)$
$n = 1$	-0.692	0.526	5.18
$n = 2$	-0.790	-0.588	5.18
$n = 3$	-0.300	0.218	5.18

Table 7: Fit parameters of f_T^n , f_{T+}^n , f_{T-}^n , and $f_{T_0}^n$ form factors for 3P_2 states in eq. (48).

f_1^n			
State	F_0	a	b
$n = 1$	0.323	2.98	-0.514
$n = 2$	0.210	1.40	-2.03
$n = 3$	0.119	0.407	0.0532

f_2^n			
State	F_0	a	b
$n = 1$	-0.332	2.49	0.262
$n = 2$	-0.228	3.22	0.682
$n = 3$	-0.139	1.43	0.110

Table 8: Fit parameters of f_1^n and f_2^n form factors for 3P_0 states in eq. (49).

f_V^n			
State	F_0	a	b
$n = 1$	0.229	6.91	7.06
$n = 2$	0.231	2.02	0.348
$n = 3$	0.368	3.69	2.75

f_{V+}^n			
State	F_0	a	b
$n = 1$	0.291	2.41	-1.82
$n = 2$	0.274	1.44	-2.08
$n = 3$	0.431	1.32	5.93

f_{V-}^n			
State	F_0	a	b
$n = 1$	0.397	4.07	3.89
$n = 2$	0.418	2.45	1.97
$n = 3$	0.530	2.89	1.60

$f_{V_0}^n$			
State	F_0	a	b
$n = 1$	-0.141	2.70	4.69
$n = 2$	-0.106	2.23	4.05
$n = 3$	-0.116	2.23	2.24

Table 9: Fit parameters of f_V^n , f_{V+}^n , f_{V-}^n , and $f_{V_0}^n$ form factors for 1P_1 states in eq. (49).

f_V^n			
State	F_0	a	b
$n = 1$	-0.966	4.63	3.03
$n = 2$	-0.918	1.81	-0.625
$n = 3$	-0.621	1.68	0.00820

f_{V+}^n			
State	F_0	a	b
$n = 1$	-0.666	2.12	0.955
$n = 2$	-0.633	2.34	0.157
$n = 3$	-0.476	1.95	0.741

f_{V-}^n			
State	F_0	a	b
$n = 1$	0.249	2.02	0.213
$n = 2$	0.180	0.976	-6.27
$n = 3$	0.0320	-3.37	-5.93

$f_{V_0}^n$			
State	F_0	a	b
$n = 1$	0.0501	2.86	6.18
$n = 2$	0.0234	2.20	1.40
$n = 3$	0.0343	2.73	-0.808

Table 10: Fit parameters of f_V^n , f_{V+}^n , f_{V-}^n , and $f_{V_0}^n$ form factors for 3P_1 states in eq. (49).

f_T^n					$f_{T_+}^n = -f_{T_-}^n$				
State	F_0	a	b	$m_{fit} (GeV)$	State	F_0	a	b	$m_{fit} (GeV)$
$n = 1$	-0.118	5.57	3.36	6.93	$n = 1$	0.0818	2.85	1.33	5.82
$n = 2$	-0.157	4.22	1.87	6.62	$n = 2$	0.0985	2.88	0.343	6.38
$n = 3$	-0.151	2.90	0.224	6.17	$n = 3$	-0.0640	1.94	1.55	7.08

$f_{T_0}^n$				
State	F_0	a	b	$m_{fit} (GeV)$
$n = 1$	-0.170	2.86	2.29	6.96
$n = 2$	-0.209	2.75	1.55	7.30
$n = 3$	-0.102	2.39	1.52	7.38

Table 11: Fit parameters of f_T^n , $f_{T_+}^n$, $f_{T_-}^n$, and $f_{T_0}^n$ form factors for 3P_2 states in eq. (49).

References

- [1] R. Aaij *et al.* [LHCb], Phys. Rev. D **90** (2014) no.3, 032009 doi:10.1103/PhysRevD.90.032009 [arXiv:1407.2126 [hep-ex]].
- [2] R. Aaij *et al.* [LHCb], Phys. Rev. Lett. **120** (2018) no.12, 121801 doi:10.1103/PhysRevLett.120.121801 [arXiv:1711.05623 [hep-ex]].
- [3] S. Godfrey and N. Isgur, Phys. Rev. D **32** (1985), 189-231 doi:10.1103/PhysRevD.32.189
- [4] F. Abe *et al.* [CDF], Phys. Rev. D **58** (1998), 112004 doi:10.1103/PhysRevD.58.112004 [arXiv:hep-ex/9804014 [hep-ex]].
- [5] T. Aliev and M. Savci, Phys. Lett. B **480**, 97-104 (2000) doi:10.1016/S0370-2693(00)00378-6 [arXiv:hep-ph/9908203 [hep-ph]].
- [6] T. Aliev and M. Savci, Eur. Phys. J. C **47**, 413-421 (2006) doi:10.1140/epjc/s2006-02579-5 [arXiv:hep-ph/0601267 [hep-ph]].
- [7] K. Azizi and V. Bashiry, Phys. Rev. D **76**, 114007 (2007) doi:10.1103/PhysRevD.76.114007 [arXiv:0708.2068 [hep-ph]].
- [8] X. W. Kang, T. Luo, Y. Zhang, L. Y. Dai and C. Wang, Eur. Phys. J. C **78** (2018) no.11, 909 doi:10.1140/epjc/s10052-018-6385-9 [arXiv:1808.02432 [hep-ph]].
- [9] N. Ghahramany, R. Khosravi and K. Azizi, Phys. Rev. D **78**, 116009 (2008) doi:10.1103/PhysRevD.78.116009 [arXiv:0811.2674 [hep-ph]].
- [10] K. Azizi, F. Falahati, V. Bashiry and S. Zebarjad, Phys. Rev. D **77**, 114024 (2008) doi:10.1103/PhysRevD.77.114024 [arXiv:0806.0583 [hep-ph]].
- [11] T. Aliev and M. Savci, Phys. Lett. B **434**, 358-364 (1998) doi:10.1016/S0370-2693(98)00692-3 [arXiv:hep-ph/9804407 [hep-ph]].
- [12] T. Aliev and M. Savci, J. Phys. G **24**, 2223-2228 (1998) doi:10.1088/0954-3899/24/12/006 [arXiv:hep-ph/9805239 [hep-ph]].
- [13] K. Azizi, R. Khosravi and V. Bashiry, Eur. Phys. J. C **56**, 357-370 (2008) doi:10.1140/epjc/s10052-008-0668-5 [arXiv:0805.2806 [hep-ph]].
- [14] K. Azizi and R. Khosravi, Phys. Rev. D **78**, 036005 (2008) doi:10.1103/PhysRevD.78.036005 [arXiv:0806.0590 [hep-ph]].
- [15] D. s. Du and Z. Wang, Phys. Rev. D **39** (1989), 1342 doi:10.1103/PhysRevD.39.1342
- [16] S. S. Gershtein, V. V. Kiselev, A. K. Likhoded and A. V. Tkabladze, Phys. Usp. **38** (1995), 1-37 doi:10.1070/PU1995v03n01ABEH000063 [arXiv:hep-ph/9504319 [hep-ph]].
- [17] C. F. Qiao, P. Sun, D. Yang and R. L. Zhu, Phys. Rev. D **89** (2014) no.3, 034008 doi:10.1103/PhysRevD.89.034008 [arXiv:1209.5859 [hep-ph]].

- [18] A. Esposito, A. L. Guerrieri, F. Piccinini, A. Pilloni and A. D. Polosa, Int. J. Mod. Phys. A **30** (2015), 1530002 doi:10.1142/S0217751X15300021 [arXiv:1411.5997 [hep-ph]].
- [19] D. L. Canham, H. W. Hammer and R. P. Springer, Phys. Rev. D **80** (2009), 014009 doi:10.1103/PhysRevD.80.014009 [arXiv:0906.1263 [hep-ph]].
- [20] Z. F. Sun, M. Bayar, P. Fernandez-Soler and E. Oset, Phys. Rev. D **93** (2016) no.5, 054028 doi:10.1103/PhysRevD.93.054028 [arXiv:1510.06316 [hep-ph]].
- [21] X. W. Kang and J. A. Oller, Eur. Phys. J. C **77** (2017) no.6, 399 doi:10.1140/epjc/s10052-017-4961-z [arXiv:1612.08420 [hep-ph]].
- [22] M. A. Shifman, A. I. Vainshtein and V. I. Zakharov, Nucl. Phys. B **147** (1979), 385-447 doi:10.1016/0550-3213(79)90022-1
- [23] R. Alkofer and L. von Smekal, Phys. Rept. **353** (2001), 281 doi:10.1016/S0370-1573(01)00010-2 [arXiv:hep-ph/0007355 [hep-ph]].
- [24] W. J. Marciano and H. Pagels, Phys. Rept. **36** (1978), 137 doi:10.1016/0370-1573(78)90208-9
- [25] I. I. Y. Bigi, N. G. Uraltsev and A. I. Vainshtein, Phys. Lett. B **293** (1992), 430-436 [erratum: Phys. Lett. B **297** (1992), 477-477] doi:10.1016/0370-2693(92)90908-M [arXiv:hep-ph/9207214 [hep-ph]].
- [26] V. V. Kiselev, A. K. Likhoded and A. I. Onishchenko, Nucl. Phys. B **569** (2000), 473-504 doi:10.1016/S0550-3213(99)00505-2 [arXiv:hep-ph/9905359 [hep-ph]].
- [27] K. Azizi, H. Sundu and M. Bayar, Phys. Rev. D **79** (2009) 116001 doi:10.1103/PhysRevD.79.116001 [arXiv:0902.1467 [hep-ph]].
- [28] E. Cincioglu, J. Nieves, A. Ozpineci and A. U. Yilmazer, Eur. Phys. J. C **76** (2016) no.10, 576 doi:10.1140/epjc/s10052-016-4413-1 [arXiv:1606.03239 [hep-ph]].
- [29] S. J. Brodsky, H. C. Pauli and S. S. Pinsky, Phys. Rept. **301** (1998), 299-486 doi:10.1016/S0370-1573(97)00089-6 [arXiv:hep-ph/9705477 [hep-ph]].
- [30] C. W. Hwang, JHEP **0910**, 074 (2009) doi:10.1088/1126-6708/2009/10/074 [arXiv:0906.4412 [hep-ph]].
- [31] M. A. Olpak, A. Ozpineci and V. Tanriverdi, Phys. Rev. D **96**, no. 1, 014026 (2017) doi:10.1103/PhysRevD.96.014026 [arXiv:1608.04539 [hep-ph]].
- [32] D. Leljak, B. Melic and M. Patra, JHEP **1905**, 094 (2019) doi:10.1007/JHEP05(2019)094 [arXiv:1901.08368 [hep-ph]].
- [33] D. Ebert, R. N. Faustov and V. O. Galkin, Phys. Rev. D **82**, 034019 (2010) doi:10.1103/PhysRevD.82.034019 [arXiv:1007.1369 [hep-ph]].
- [34] M. A. Ivanov, J. G. Korner and P. Santorelli, Phys. Rev. D **71** (2005), 094006 [erratum: Phys. Rev. D **75** (2007), 019901] doi:10.1103/PhysRevD.75.019901 [arXiv:hep-ph/0501051 [hep-ph]].

- [35] R. N. Faustov, V. O. Galkin and X. W. Kang, Phys. Rev. D **101** (2020) no.1, 013004 doi:10.1103/PhysRevD.101.013004 [arXiv:1911.08209 [hep-ph]].
- [36] A. Issadykov, M. A. Ivanov and G. Nurbakova, EPJ Web Conf. **158** (2017) 03002 doi:10.1051/epjconf/201715803002 [arXiv:1907.13210 [hep-ph]].
- [37] F. S. Navarra, M. Nielsen, M. E. Bracco, M. Chiapparini and C. L. Schat, Phys. Lett. B **489** (2000), 319-328 doi:10.1016/S0370-2693(00)00967-9 [arXiv:hep-ph/0005026 [hep-ph]].
- [38] M. E. Bracco, M. Chiapparini, A. Lozea, F. S. Navarra and M. Nielsen, Phys. Lett. B **521** (2001), 1-6 doi:10.1016/S0370-2693(01)01192-3 [arXiv:hep-ph/0108223 [hep-ph]].
- [39] R. D. Matheus, F. S. Navarra, M. Nielsen and R. Rodrigues da Silva, Phys. Lett. B **541** (2002), 265-272 doi:10.1016/S0370-2693(02)02259-1 [arXiv:hep-ph/0206198 [hep-ph]].
- [40] F. S. Navarra, M. Nielsen and M. E. Bracco, Phys. Rev. D **65** (2002), 037502 doi:10.1103/PhysRevD.65.037502 [arXiv:hep-ph/0109188 [hep-ph]].
- [41] M. E. Bracco, M. Chiapparini, F. S. Navarra and M. Nielsen, Phys. Lett. B **605** (2005), 326-334 doi:10.1016/j.physletb.2004.11.024 [arXiv:hep-ph/0410071 [hep-ph]].
- [42] F. Carvalho, F. O. Duraes, F. S. Navarra and M. Nielsen, Phys. Rev. C **72** (2005), 024902 doi:10.1103/PhysRevC.72.024902 [arXiv:hep-ph/0508137 [hep-ph]].
- [43] R. D. Matheus, F. S. Navarra, M. Nielsen and R. Rodrigues da Silva, Int. J. Mod. Phys. E **14** (2005), 555-567 doi:10.1142/S0218301305003399
- [44] B. Osorio Rodrigues, M. E. Bracco, M. Nielsen and F. S. Navarra, Nucl. Phys. A **852** (2011), 127-140 doi:10.1016/j.nuclphysa.2011.01.001 [arXiv:1003.2604 [hep-ph]].
- [45] M. E. Bracco, M. Chiapparini, F. S. Navarra and M. Nielsen, Prog. Part. Nucl. Phys. **67** (2012), 1019-1052 doi:10.1016/j.ppnp.2012.03.002 [arXiv:1104.2864 [hep-ph]].
- [46] M. E. Bracco, M. Chiapparini, F. S. Navarra and M. Nielsen, Phys. Lett. B **659** (2008), 559-564 doi:10.1016/j.physletb.2007.11.066 [arXiv:0710.1878 [hep-ph]].
- [47] P. A. Zyla *et al.* [Particle Data Group], PTEP **2020** (2020) no.8, 083C01 doi:10.1093/ptep/ptaa104
- [48] S. Narison, Phys. Lett. B **802** (2020), 135221 doi:10.1016/j.physletb.2020.135221 [arXiv:1906.03614 [hep-ph]].
- [49] E. Hernandez, J. Nieves and J. M. Verde-Velasco, Phys. Rev. D **74**, 074008 (2006) doi:10.1103/PhysRevD.74.074008 [arXiv:hep-ph/0607150 [hep-ph]].
- [50] P. Ball and V. M. Braun, Phys. Rev. D **54** (1996), 2182-2193 doi:10.1103/PhysRevD.54.2182 [arXiv:hep-ph/9602323 [hep-ph]].
- [51] V. M. Braun and N. Kivel, Phys. Lett. B **501** (2001), 48-53 doi:10.1016/S0370-2693(01)00095-8 [arXiv:hep-ph/0012220 [hep-ph]].

- [52] H. Y. Cheng, Y. Koike and K. C. Yang, Phys. Rev. D **82** (2010), 054019 doi:10.1103/PhysRevD.82.054019 [arXiv:1007.3541 [hep-ph]].
- [53] X. X. Wang, W. Wang and C. D. Lu, Phys. Rev. D **79** (2009), 114018 doi:10.1103/PhysRevD.79.114018 [arXiv:0901.1934 [hep-ph]].
- [54] M. A. Ivanov, J. G. Korner and P. Santorelli, Phys. Rev. D **73** (2006), 054024 doi:10.1103/PhysRevD.73.054024 [arXiv:hep-ph/0602050 [hep-ph]].
- [55] D. Ebert, R. N. Faustov and V. O. Galkin, Phys. Rev. D **67** (2003), 014027 doi:10.1103/PhysRevD.67.014027 [arXiv:hep-ph/0210381 [hep-ph]].
- [56] V. V. Braguta, A. K. Likhoded and A. V. Luchinsky, Phys. Rev. D **79**, 074004 (2009) doi:10.1103/PhysRevD.79.074004 [arXiv:0810.3607 [hep-ph]].